Planet Simulator

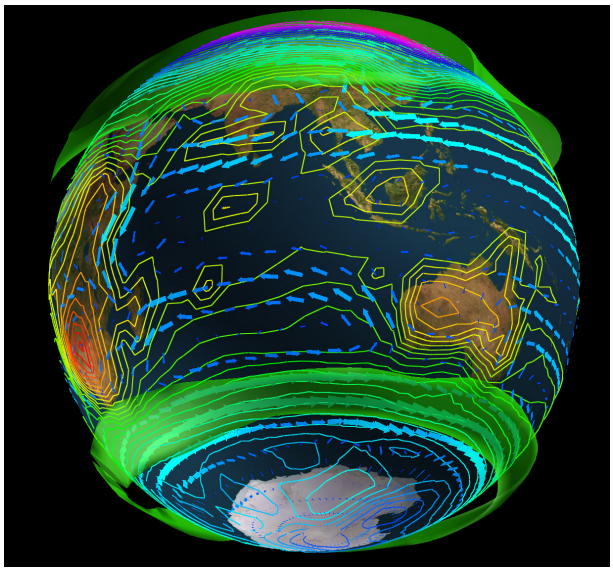

Reference Manual

Version 15.0

F. Lunkeit M. Böttinger K. Fraedrich H. Jansen E. Kirk
A. Kleidon U. Luksch

July 18, 2007

Contents

1 Preface **5**

I Atmosphere: PUMA II **7**

2 Model Dynamics **9**
2.1 A dimensionless set of differential equations 9
2.2 Mode splitting 10
2.3 Numerics 11
2.3.1 Spectral Transform method 11
2.3.2 Vertical discretization 12
2.3.3 Semi-implicit time stepping 13

3 Model Physics - Parameterizations **15**
3.1 Surface Fluxes and Vertical Diffusion 15
3.1.1 Surface Fluxes 15
3.1.2 Vertical Diffusion 17
3.2 Horizontal Diffusion 19
3.3 Radiation 20
3.3.1 Short Wave Radiation 20
3.3.2 Long Wave Radiation 25
3.3.3 Ozone 28
3.3.4 Additional Newtonian cooling 29
3.4 Moist Processes and Dry Convection 30
3.4.1 Correction of Negative Humidity 30
3.4.2 Saturation Specific Humidity 30
3.4.3 Cumulus Convection 30
3.4.4 Large Scale Precipitation 33
3.4.5 Cloud Formation 33
3.4.6 Evaporation of Precipitation and Snow Fall 34
3.4.7 Dry Convective Adjustment 35
3.5 Land Surface and Soil 36
3.5.1 Temperatures 36
3.5.2 Soil Hydrology 37
3.5.3 River Transport 38
3.5.4 Other Land Surface Parameter 39
3.6 Sea Surface 39
3.7 References 41

4 Equations **43**
4.1 Pressure coordinate . . . 43
4.2 Sigma-system . . . 43
4.3 Matrix B . . . 44

II Ocean: Mixed Layer 47

5 Slab Ocean Model **49**
5.1 Constant-depth mixed layer and flux correction . . . 49
5.2 Kraus-Turner type model . . . 49

III Biosphere: SIMBA 53

6 Dynamic Vegetation **55**
6.1 Vegetative Cover . . . 55
6.2 Carbon Balance . . . 56
6.3 Derivation of Land Surface Parameters . . . 56
6.4 Model Calibration . . . 56

IV Ice 59

7 Model Description **61**

V Bibliography 71

Chapter 1

Preface

For two decades, a comprehensive, three-dimensional global atmospheric general circulation model (GCM) is being provided by the National Center for Atmospheric Research (NCAR, Climate and Global Dynamics Division) to university and other scientists for use in analysing and understanding the global climate. Designed as a Community Climate Model (CCM) it has been continuously developed since. Other centres have also constructed comprehensive climate models of similarly high complexity, mostly for their research interests.

As the complexity of general circulation models has been and still is growing considerably, it is not surprising that, for both education and research, models simpler than those comprehensive GCMs at the cutting edge of the development, are becoming more and more attractive. These medium complexity models do not simply enhance the climate model hierarchy. They support understanding atmospheric or climate phenomena by simplifying the system gradually to reveal the key mechanisms. They also provide an ideal tool kit for students to be educated and to teach themselves, gaining practice in model building or modeling. Our aim is to provide such a model of intermediate complexity for the university environment: the PlanetSimulator. It can be used for training the next GCM developers, to support scientists to understand climate processes, and to do fundamental research.

From PUMA to PlanetSimulator: Dynamical core and physical processes comprise a general circulation model (GCM) of planetary atmospheres. Stand-alone, the dynamical core is a simplified general circulation model like our Portable University Model of the Atmosphere or PUMA. Still, linear processes are introduced to run it, like Newtonian cooling and Rayleigh friction, which parameterise diabatic heating and planetary boundary layers. Though simple, PUMA has been enjoying a wide spectrum of applications and initiating collaborations in fundamental research, atmospheric dynamics and education alike. Specific applications, for example, are tests and consequences of the maximum entropy production principle, synchronisation and spatio-temporal coherence resonance, large scale dynamics of the atmospheres on Earth, Mars and Titan. Based on this experience we combined the leitmotifs behind PUMA and the Community Model, to applying, building, and coding a 'PlanetSimulator'.

Applying the PlanetSimulator in a university environment has two aspects: First, the code must be open and freely available as the software required to run it; it must be user friendly, inexpensive and equipped with a graphical user interface. Secondly, it should be suitable for teaching project studies in classes or lab, where students practice general circulation modelling, in contrast to technicians running a comprehensive GCM; that is, science versus engineering.

Building the PlanetSimulator includes, besides an atmospheric GCM of medium complexity, other compartments of the climate system, for example, an ocean with sea ice, a land surface with biosphere. Here these other compartments are reduced to linear systems. That is, not unlike PUMA as a dynamical core with linear physics, the PlanetSimulator consists of a GCM with, for example, a linear ocean/sea-ice module formulated in terms of a mixed layer energy

balance. The soil/biosphere module is introduced analoguously. Thus, working the Planet-Simulator is like testing the performance of an atmospheric or oceanic GCM interacting with various linear processes, which parameterise the variability of the subsystems in terms of their energy (and mass) balances.

Coding the PlanetSimulator requires that it is portable to many platforms ranging from personal computers over workstations to mainframes; massive parallel computers and clusters of networked machines are also supported. The system is scalable with regard to vertical and horizontal resolutions, provides experiment dependent model configurations, and it has a transparent and rich documented code.

Acknowledgement: The development of the Planet Simulator was generously granted by the German Federal Ministry for Education and Research (BMBF) during the years 2000 - 2003.

Part I

Atmosphere: PUMA II

Chapter 2

Model Dynamics

The primitive equations, which represent the dynamical core of the atmospheric model, consist of the conservation of momentum and mass, the first law of thermodynamics and the equation of state, simplified by the hydrostatic approximation.

2.1 A dimensionless set of differential equations

The prognostic equations for the horizontal velocities are transformed into equations of the vertical component of the vorticity ζ and the divergence D. A vertical coordinate system where the lower boundary exactly coincides with a coordinate surface is defined by σ (the pressure normalized by the surface pressure). Latitude φ and longitude λ represent the horizontal coordinates and the poleward convergence of the meridians is explicitly introduced re-writing the zonal (u) and meridional (ν) velocities: $U = u\cos\varphi$, $V = \nu\cos\varphi$ and $\mu = \sin\varphi$. The implicitly treated gravity wave terms are linearized about a reference profile T_0. Therefore, prognostic equation for temperature deviations $T' = T - T_0$ are derived; we use a constant reference temperature $T_0 = 250K$ for all σ levels. The turbulent flux divergences due to prior Reynolds averaging enter the dynamic and thermodynamic equations as parameterizations formally included in the terms: P_ζ, P_D, P_T.

A dimensionless set of differential equations is derived by scaling vorticity ζ and divergence D by angular velocity of the earth Ω, pressure p by a constant surface pressure p_s, temperatures T and T' by $a^2\Omega^2/R$ and the orography and geopotential ψ by $a^2\Omega^2/g$ (g is the acceleration of gravity and R the gas constant for dry air). The dimensionless primitive equations in the (λ, μ, σ)-coordinates [Hoskins and Simmons (1975)] are given by

Conservation of momentum (vorticity and divergence equation)

$$\frac{\partial \zeta + f}{\partial t} = \frac{1}{(1-\mu^2)}\frac{\partial F_\nu}{\partial \lambda} - \frac{\partial F_u}{\partial \mu} + P_\zeta \tag{2.1}$$

$$\frac{\partial D}{\partial t} = \frac{1}{(1-\mu^2)}\frac{\partial F_u}{\partial \lambda} + \frac{\partial F_\nu}{\partial \mu} - \nabla^2 E - \nabla^2(\phi + T_0 \ln p_s) + P_D \tag{2.2}$$

Hydrostatic approximation (using the equation of state)

$$0 = \frac{\partial \phi}{\partial \ln \sigma} + T \tag{2.3}$$

Conservation of mass (continuity equation)

$$\frac{\partial \ln p_s}{\partial t} = -\int_0^1 A d\sigma \tag{2.4}$$

Thermodynamic equation

$$\frac{\partial T'}{\partial t} = F_T - \dot{\sigma}\frac{\partial T}{\partial \sigma} + \kappa W T + \frac{J}{c_p} + P_T \tag{2.5}$$

with the notations

$$F_u = (\zeta + f)V - \dot{\sigma}\frac{\partial U}{\partial \sigma} - T'\frac{\partial \ln p_s}{\partial \lambda}$$
$$F_\nu = -(\zeta + f)U - \dot{\sigma}\frac{\partial V}{\partial \sigma} - (1-\mu^2)T'\frac{\partial \ln p_s}{\partial \mu}$$
$$F_T = -\frac{1}{(1-\mu^2)}\frac{\partial (UT')}{\partial \lambda} - \frac{\partial (VT')}{\partial \mu} + DT'$$
$$E = \frac{U^2 + V^2}{2(1-\mu^2)}$$
$$\dot{\sigma} = \sigma \int_0^1 A d\sigma - \int_0^\sigma A d\sigma$$
$$W = \frac{\omega}{p} = \vec{V}\cdot\nabla \ln p_s - \frac{1}{\sigma}\int_0^\sigma A d\sigma$$
$$A = D + \vec{V}\cdot\nabla \ln p_s = \tfrac{1}{p_s}\nabla \cdot p_s \vec{V}.$$

Here is $\dot{\sigma}$ the vertical velocity in the σ system, J the diabatic heating per unit mass and E the kinetic energy per unit mass. The streamfunction ψ and the velocity potential χ represent the nondivergent and the irrotational part of the velocity field
$U = -(1-\mu^2)\frac{\partial \psi}{\partial \mu} + \frac{\partial \chi}{\partial \lambda}$ and $V = \frac{\partial \psi}{\partial \lambda} + (1-\mu^2)\frac{\partial \chi}{\partial \mu}$ with $\zeta = \nabla^2\psi$ and $D = \nabla^2\chi$.

2.2 Mode splitting

The fast gravity wave modes are linearized around a reference temperature profile $\vec{T_0}$. Now, the differential equations (2.1-2.5) can be separated into fast (linear) gravity modes and the slower non-linear terms (N_D, N_p, N_T). The linear terms of the equations contain the effect of the divergence (or the gravity waves) on the surface pressure tendency, the temperature tendency and the geopotential. A discussion of the impact of the reference profile on the stability of the semi-implicit numerical scheme is presented by [Simmons et al.(1978)].

$$\frac{\partial D}{\partial t} = N_D - \bigtriangledown^2(\phi + T_0 \ln p_s) \tag{2.6}$$

$$\frac{\partial \phi}{\partial \ln \sigma} = -T \tag{2.7}$$

$$\frac{\partial \ln p_s}{\partial t} = N_p - \int_0^1 D d\sigma \tag{2.8}$$

$$\frac{\partial T'}{\partial t} = N_T - \dot{\sigma}_L \frac{\partial T_0}{\partial \sigma} + \kappa W_L T_0 \tag{2.9}$$

with the non-linear terms

$$N_D = \frac{1}{(1-\mu^2)}\frac{\partial F_u}{\partial \lambda} + \frac{F_\nu}{\partial \mu} - \bigtriangledown^2 E + P_D$$

$$N_p = -\int_0^1 [A-D]d\sigma$$

$$N_T = F_T - \dot{\sigma}_N \frac{\partial T_0}{\partial \sigma} - \dot{\sigma}\frac{\partial T'}{\partial \sigma} + \kappa W_N T_0 + \kappa W T' + \frac{J}{c_p} + P_T$$

and the notations

$$\dot{\sigma}_L = \sigma \int_0^1 D d\sigma - \int_0^\sigma D d\sigma$$

$$\dot{\sigma}_N = \sigma \int_0^1 [A-D]d\sigma - \int_0^\sigma [A-D]d\sigma$$

$$W_L = -\frac{1}{\sigma}\int_0^\sigma D d\sigma$$

$$W_N = \vec{V}\cdot\nabla \ln p_s - \frac{1}{\sigma}\int_0^\sigma [A-D]d\sigma$$

$$A - D = \vec{V}\cdot\nabla \ln p_s$$

$$\dot{\sigma} = \dot{\sigma_L} + \dot{\sigma_N} = \sigma \int_0^1 A d\sigma - \int_0^\sigma A d\sigma$$

$$W = W_L + W_N = \vec{V}\cdot\nabla \ln p_s - \frac{1}{\sigma}\int_0^\sigma A d\sigma$$

The index L denote the linear and N the non-linear part in the vertical advection ($\dot{\sigma}\frac{\partial T}{\partial \sigma}$) and the adiabatic heating or cooling (κWT with $W = \frac{\omega}{p}$). The non-linear terms are solve explicitly in the physical space (on the Gaussian grid; section 2.3.1) and the linear terms are calculated implicitly in the spectral space (for the spherical harmonics; see section 2.3.1).

2.3 Numerics

Solving the equations requires a suitable numerical representation of the spatial fields and their time change. A conventional approach is spectral representation in the horizontal using the transform method, finite differences in the vertical, and a semi-implicit time stepping.

2.3.1 Spectral Transform method

The spectral method used in the computation of the nonlinear terms involves storing of a large number of so-called interaction coefficients, the number of which increases very fast with increasing resolution. The computing time and storing space requirements exceed all practical limits for high resolution models. Furthermore, there are problems to incorporate locally dependent physical processes, such as release of precipitation or a convective adjustment. Therefore, the equa-

tions are solved using the spectral transform method [Orszag (1970), Eliassen et al. (1970)]. This method uses an auxiliary grid in the physical space where point values of the dependent variables are computed.

The prognostic variables are represented in the horizontal by truncated series of spherical harmonics (Q stands for ζ, D, T and $\ln p_s$)

$$Q(\lambda,\mu,\sigma,t) = \sum_{m=-M}^{M} \sum_{n=|m|}^{M} Q_n^m(\sigma,t) P_n^m(\mu) e^{im\lambda} \tag{2.10}$$

$$= Q_n^0(\sigma,t)P_n^0(\mu) + 2\sum_{m=1}^{M}\sum_{n=m}^{M} Q_n^m(\sigma,t)P_n^m(\mu)e^{im\lambda}$$

For each variable the spectral coefficient is defined by

$$Q_n^m(\sigma,t) = \frac{1}{4\pi}\int_{-1}^{1}\int_{0}^{2\pi} Q(\lambda,\mu,\sigma,t)P_n^m(\mu)e^{-im\lambda}d\lambda d\mu \tag{2.11}$$

The spectral coefficients $Q_n^m(\sigma,t)$ are obtained by Gaussian quadrature of the Fourier coefficients F^m at each latitude φ which are calculated by Fast Fourier Transformation with
$F^m(\mu,\sigma,t) = \frac{1}{4\pi}\int_0^{2\pi} Q(\lambda,\mu,\sigma,t)e^{-im\lambda}d\lambda$
The auxiliary grid in the physical space (Gaussian grid) is defined by M_g equally spaced longitudes and J_g Gaussian latitudes with $M_g \geq 3M+1$ and $J_g \geq 0.5(3M+1)$.

2.3.2 Vertical discretization

The prognostic variables vorticity, temperature and divergence are calculated at full levels and the vertical velocity at half levels. Therefore, the vertical advection for the level r is calculated (Q stands for ζ, D, T and $\ln p_s$)

$$(\dot\sigma\frac{\partial Q}{\partial\sigma})\hat{=}\frac{1}{2\Delta\sigma_r}[\dot\sigma_{r+0.5}(Q_{r+1}-Q_r)+\dot\sigma_{r-0.5}(Q_r-Q_{r-1})] \tag{2.12}$$

For the hydrostatic approximation (3) an angular momentum conserving finite-difference scheme [Simmons and Burridge (1981)] is used which solves the equation at half levels ($r+0.5; r=1,...,n; n=$ number of levels)

$$\frac{\partial\phi}{\partial\ln\sigma} + T\hat{=}\phi_{r+0.5}-\phi_{r-0.5}+T_r\cdot\ln\frac{\sigma_{r+0.5}}{\sigma_{r-0.5}} \tag{2.13}$$

Full level values (r) of geopotential are given by

$$\phi_r = \phi_{r+0.5} + \alpha_r T_r \tag{2.14}$$

with $\alpha_r = 1 - \frac{\sigma_{r-0.5}}{\Delta\sigma_r}\ln\frac{\sigma_{r+0.5}}{\sigma_{r-0.5}}$ and $\Delta\sigma_r = \sigma_{r+0.5}-\sigma_{r-0.5}$

2.3.3 Semi-implicit time stepping

Sound waves are filtered by the hydrostatic approximation (filter for vertical sound waves) and the lower boundary condition in pressure or sigma-coordinates (vanishing vertical velocity at the surface, i.e. the total derivative of the surface pressure is zero; filter for horizontal sound waves). But the fast propagation of the gravity waves strongly reduce the time step of explicit numerical schemes, therefore mode splitting is used (section 2.2) and an implicit scheme for the divergence is applied (see below). The vorticity equation is computed by an explicit scheme (leap frog) and the common Robert/Asselin time filter is used [Haltiner and Williams (1982)].

The implicit formulation for the divergence is derived using the conservation of mass, the hydrostatic approximation and the thermodynamic equation (eq. 2.6-2.9) approximated by its finite difference analogues in time (t) using the notation (for each variable D, T, $\ln p_s$, and ϕ)

$$\delta_t Q = \frac{Q^{t+\Delta t} - Q^{t-\Delta t}}{2\Delta t} \qquad \text{and} \qquad \overline{Q}^t = 0.5(Q^{t+\Delta t} + Q^{t-\Delta t}) = Q^{t-\Delta t} + \Delta t \delta_t Q$$

The divergence is calculated by the non-linear term at time step t and the linearized term which is a function of the geopotential (or the temperature tendency) and the surface pressure tendency.

$$\delta_t D = {N_D}^t - \bigtriangledown^2(\overline{\phi}^t + T_0[\ln p_s^{t-\Delta t} + \Delta t\ \delta_t \ln p_s]) \tag{2.15}$$

$$\overline{\phi - \phi_s}^t = L_\phi[T^{t-\Delta t} + \Delta t \delta_t T] = L_\phi[T^{t-\Delta t} + \Delta t\ \delta_t T'] \tag{2.16}$$

$$\delta_t \ln p_s = {N_p}^t - L_p[D^{t-\Delta t} + \Delta t\ \delta_t D] \tag{2.17}$$

$$\delta_t T' = {N_T}^t - L_T[D^{t-\Delta t} + \Delta t\ \delta_t D] \tag{2.18}$$

The implicit formulation of the divergence equation is derived from the finite difference analogues of the new time step $t + \Delta t$ applied for each level r ($r = 1, ...n$) which can also formulated as a vector $\vec{D}$ with the n components.

$$\begin{pmatrix} 1 - b_{11} & b_{21} & \cdots & b_{n1} \\ b_{12} & 1 - b_{22} & \ddots & \vdots \\ \vdots & \vdots & \ddots & \vdots \\ b_{1n} & b_{2n} & \cdots & 1 - b_{nn} \end{pmatrix} \begin{pmatrix} D_1^{t+\Delta t} \\ D_2^{t+\Delta t} \\ \vdots \\ D_n^{t+\Delta t} \end{pmatrix} = \begin{pmatrix} D_1^{t-\Delta t} \\ D_2^{t-\Delta t} \\ \vdots \\ D_n^{t-\Delta t} \end{pmatrix} + 2\Delta t \begin{pmatrix} R_1 \\ R_2 \\ \vdots \\ R_n \end{pmatrix}$$

In matrix formulation

$$(\mathcal{I} - \mathcal{B}\Delta t^2 \bigtriangledown^2)\vec{D}^{t+\Delta t} = \vec{D}^{t-\Delta t} + 2\Delta t[\vec{N}_D - \bigtriangledown^2(\vec{\phi}^{t-\Delta t} + \vec{T}_0 \ln p_s^{t-\Delta t})]$$

$$- 2\Delta t^2 \bigtriangledown^2 (\mathcal{L}_\phi \vec{N}_T + \vec{T}_0 N_p) \tag{2.19}$$

The matrix $\mathcal{B} = \mathcal{L}_\phi \mathcal{L}_T + \vec{T}_0 \vec{L}_p = \mathcal{B}(\sigma, \kappa, \vec{T}_0)$ is constant in time. The variables $\vec{D}, \vec{T}, \vec{T}', \vec{\phi} - \vec{\phi}_s$ are represented by column vectors with values at each layer, as are also $\vec{N}_D$ and $\vec{N}_T$. $\mathcal{L}_\phi$ and $\mathcal{L}_T$ are constant matrices, $\vec{L}_p$ is a row vector (see Appendix C). The matrix $\mathcal{B}$ can be calculated

seperately for each spectral coefficient because in the linearized part the spectral modes are independent of each other.

$$(\vec{D}_n^m)^{t+\Delta t} = (\mathcal{I} + \mathcal{B}\Delta t^2 c_n)^{-1}[(\vec{D}_n^m)^{t-\Delta t} + 2\Delta t\vec{R}] \tag{2.20}$$

$$(\vec{D}_n^m)^{t+\Delta t} = (\frac{\mathcal{I}}{c_n} + \mathcal{B}\Delta t^2)^{-1}[\frac{1}{c_n}(\vec{D}_n^m)^{t-\Delta t} + \frac{2\Delta t}{c_n}\vec{R}] \tag{2.21}$$

with $\bigtriangledown^2(P_n^m(\mu)e^{-im\lambda}) = -n(n+1)P_n^m(\mu)e^{-im\lambda} = -c_n P_n^m(\mu)e^{-im\lambda}$.

Chapter 3

Model Physics - Parameterizations

3.1 Surface Fluxes and Vertical Diffusion

3.1.1 Surface Fluxes

The bulk aerodynamic formulas are used to parameterize surface fluxes of zonal and meridional momentum (wind stress) F_u and F_v, sensible heat F_T and latent heat $L\,F_q$, where F_q is the surface flux of moisture and L is the latent heat of vaporisation L_v, or, depending on temperature, the latent heat of sublimation L_s:

$$\begin{aligned} F_u &= \rho\, C_m\, |\vec{v}|\, u \\ F_v &= \rho\, C_m\, |\vec{v}|\, v \\ F_T &= c_p\, \rho\, C_h\, |\vec{v}|\, (\gamma T - T_S) \\ L\, F_q &= L\, \rho\, C_h\, C_w\, |\vec{v}|\, (\delta q - q_S) \end{aligned} \tag{3.1}$$

All fluxes are positive in downward direction. ρ denotes the density, c_p is the specific heat for moist air at constant pressure ($c_p = c_{pd}\,[1 + (c_{pv}/c_{pd} - 1)\,q]$, where c_{pd} and c_{pv} are the specific heats at constant pressure for dry air and water vapor, respectively). C_m is the drag coefficient, C_h is the transfer coefficient for heat, T_S is the surface temperature, q_S is the surface specific humidity and $|\vec{v}|$ is the absolute value of the horizontal velocity at the lowermost level. The wetness factor C_w accounts for different evaporation efficiencies due to surface characteristics (Section 3.5.2). u, v, T and q are the zonal and meridional wind components, the temperature and the specific humidity, respectively, of the lowermost model level. The factors γ and δ are used to relate the model quantities to the respective near surface values. δ is set to 1 and γ is set to give a potential temperature:

$$\gamma = \left(\frac{p_S}{p}\right)^{\frac{R_d}{c_{pd}}} \tag{3.2}$$

where p is the pressure of the lowermost model level, p_S is the surface pressure and R_d is the gas constant for dry air.

While γ, ρ, C_m, C_h, $|\vec{v}|$, T_S and q_S apply to time level $t - \Delta t$, values for $u^{t+\Delta t}$, $v^{t+\Delta t}$, $T^{t+\Delta t}$ and $q^{t+\Delta t}$ are computed implicitly from the discretized tendency equations:

$$
\begin{aligned}
\frac{u^{t+\Delta t} - u^{t-\Delta t}}{2\Delta t} &= -\frac{1}{\rho\,\Delta z}\,F_u^{t+\Delta t} &&= -\frac{g\,\rho\,C_m\,|\vec{v}|}{p_S\,\Delta\sigma}\,u^{t+\Delta t} \\
\frac{v^{t+\Delta t} - v^{t-\Delta t}}{2\Delta t} &= -\frac{1}{\rho\,\Delta z}\,F_v^{t+\Delta t} &&= -\frac{g\,\rho\,C_m\,|\vec{v}|}{p_S\,\Delta\sigma}\,v^{t+\Delta t} \\
\frac{T^{t+\Delta t} - T^{t-\Delta t}}{2\Delta t} &= -\frac{1}{c_p\,\rho\,\Delta z}\,F_T^{t+\Delta t} &&= -\frac{g\,\rho\,C_h\,|\vec{v}|}{p_S\,\Delta\sigma}\,(\gamma T^{t+\Delta t} - T_S) \\
\frac{q^{t+\Delta t} - q^{t-\Delta t}}{2\Delta t} &= -\frac{1}{\rho\,\Delta z}\,F_q^{t+\Delta t} &&= -\frac{g\,\rho\,C_h\,C_w\,|\vec{v}|}{p_S\,\Delta\sigma}\,(\delta q^{t+\Delta t} - q_S)
\end{aligned}
\tag{3.3}
$$

where g is the gravitational acceleration and $\Delta\sigma = \Delta p / p_S$ is the thickness of the lowermost model layer.

In addition to the tendencies, the surface fluxes of momentum, sensible and latent heat and the partial derivative of the sensible and the latent heat flux with respect to the surface temperature are computed:

$$
\begin{aligned}
F_u &= \rho\,C_m\,|\vec{v}|\,u^{t+\Delta t} \\
F_v &= \rho\,C_m\,|\vec{v}|\,v^{t+\Delta t} \\
F_T &= c_p\,\rho\,C_h\,|\vec{v}|\,(\gamma T^{t+\Delta t} - T_S) \\
L\,F_q &= L\,\rho\,C_h\,C_w\,|\vec{v}|\,(\delta q^{t+\Delta t} - q_S) \\
\frac{\partial F_T}{\partial T_S} &= -c_p\,\rho\,C_h\,|\vec{v}| \\
\frac{\partial (L\,F_q)}{\partial T_S} &= -L\,\rho\,C_h\,C_w\,|\vec{v}|\,\frac{\partial q_S(T_S)}{\partial T_S}
\end{aligned}
\tag{3.4}
$$

The derivatives of the fluxes may be used, for examples, for an implicit calculation of the surface temperature (see Section 3.5.1).

Drag and transfer coefficients

The calculation of the drag and the transfer coefficient C_m and C_h follows the method described in Roeckner et al. (1992) for the ECHAM-3 model, which bases on the work of Louis (1979) and Louis et al. (1982). A Richardson number dependence of C_m and C_h in accordance to the Monin-Obukhov similarity theory is given by

$$
\begin{aligned}
C_m &= \left(\tfrac{k}{\ln(z/z_0)}\right)^2 f_m(Ri, z/z_0) \\
C_h &= \left(\tfrac{k}{\ln(z/z_0)}\right)^2 f_h(Ri, z/z_0)
\end{aligned}
\tag{3.5}
$$

where k is the von Karman constant ($k = 0.4$) and z_0 is the roughness length, which depends on the surface characteristics (Section 3.5.4 and Section 3.6). The Richardson number Ri is defined as

$$
Ri = \frac{g\,\Delta z\,(\gamma_E T - \gamma_E T_S)}{\gamma T\,|\vec{v}|^2}
\tag{3.6}
$$

with γ from Eq. 3.2 and γ_E transfers temperatures to virtual potential temperatures to include the effect of moisture.

$$\gamma_E = \left(1 - \left(\frac{R_v}{R_d} - 1\right) q\right) \left(\frac{p_S}{p}\right)^{\frac{R_d}{c_{pd}}} \tag{3.7}$$

where q refers to the respective specific humidities and R_v is the gas constant for water vapor.

Different empirical formulas for stable ($Ri \geq 0$) and unstable ($Ri < 0$) situations are used. For the stable case, f_m and f_h are given by

$$\begin{aligned} f_m &= \frac{1}{1 + (2\,b\,Ri)/\sqrt{1 + d\,Ri}} \\ f_h &= \frac{1}{1 + (3\,b\,Ri)/\sqrt{1 + d\,Ri}} \end{aligned} \tag{3.8}$$

while for the unstable case, f_m and f_h are

$$\begin{aligned} f_m &= 1 - \frac{2\,b\,Ri}{1 + 3\,b\,c\,[\frac{k}{\ln(z/z_0+1)}]^2\sqrt{-Ri\,(z/z_0+1)}} \\ f_h &= 1 - \frac{3\,b\,Ri}{1 + 3\,b\,c\,[\frac{k}{\ln(z/z_0+1)}]^2\sqrt{-Ri\,(z/z_0+1)}} \end{aligned} \tag{3.9}$$

where b, c, and d are prescribed constants and set to default values of $b = 5$, $c = 5$ and $d = 5$.

3.1.2 Vertical Diffusion

Vertical diffusion representing the non resolved turbulent exchange is applied to the horizontal wind components u and v, the potential temperature θ $(= T(p_S/p)^{R_d/c_{pd}})$ and the specific humidity q. The tendencies due to the turbulent transports are given by

$$\begin{aligned} \frac{\partial u}{\partial t} &= \frac{1}{\rho}\frac{\partial J_u}{\partial z} = \frac{1}{\rho}\frac{\partial}{\partial z}(\rho\,K_m\,\frac{\partial u}{\partial z}) \\ \frac{\partial v}{\partial t} &= \frac{1}{\rho}\frac{\partial J_v}{\partial z} = \frac{1}{\rho}\frac{\partial}{\partial z}(\rho\,K_m\,\frac{\partial v}{\partial z}) \\ \frac{\partial T}{\partial t} &= \frac{1}{\rho}\frac{\partial J_T}{\partial z} = \frac{1}{\rho}\frac{\partial}{\partial z}(\rho\,K_h\,(\frac{p}{p_S})^{R_d/c_{pd}}\,\frac{\partial \theta}{\partial z}) \\ \frac{\partial q}{\partial t} &= \frac{1}{\rho}\frac{\partial J_q}{\partial z} = \frac{1}{\rho}\frac{\partial}{\partial z}(\rho\,K_h\,\frac{\partial q}{\partial z}) \end{aligned} \tag{3.10}$$

where p is the pressure, p_S is the surface pressure, R_d is the gas constant for dry air and c_{pd} is the specific heat for dry air at constant pressure. Here, the turbulent fluxes (positive downward) of zonal and meridional momentum J_u and J_v, heat $c_{pd}\,J_T$ and moisture J_q are parameterized by a linear diffusion along the vertical gradient with the exchange coefficients K_m and K_h for momentum and heat, respectively. K_m and K_h depend on the actual state (see below). As the effect of the surface fluxes are computed separately (Section 3.1.1), no flux boundary conditions for the vertical diffusion scheme are assumed at the top and the bottom

of the atmosphere but the vertical diffusion is computed starting with initial values for u, v, q and T which include the tendencies due to the surface fluxes.

As for the surface fluxes, the equations are formulated implicitely with exchange coefficients applying to the old time level. This leads to sets of linear equations for $u^{t+\Delta t}$, $v^{t+\Delta t}$, $T^{t+\Delta t}$ and $q^{t+\Delta t}$, which are solved by a back substitution method.

Exchange coefficients

The calculation of the exchange coefficient K_m and K_h follows the mixing length approach as an extension of the similarity theory used to define the drag and transfere coefficients (Section 3.1.1 and Roeckner et al. 1992):

$$\begin{aligned} K_m &= l_m^2 \left|\frac{\partial \vec{v}}{\partial z}\right| f_m(Ri) \\ K_h &= l_h^2 \left|\frac{\partial \vec{v}}{\partial z}\right| f_h(Ri) \end{aligned} \tag{3.11}$$

where the functional dependencies of f_m and f_h on Ri are the same as for C_m and C_h (Eq. 3.8 and Eq. 3.9), except that the term

$$\left[\frac{k}{\ln(z/z_0+1)}\right]^2 \sqrt{(z/z_0+1)} \tag{3.12}$$

is replaced by

$$\frac{l^2}{(\Delta z)^{3/2}\, z^{1/2}} \left[\left(\frac{z+\Delta z}{z}\right)^{1/3} - 1\right]^{3/2} \tag{3.13}$$

The Richardson number Ri is defined as

$$Ri = \frac{g}{\gamma T}\frac{\partial(\gamma_E T)}{\partial z}\left|\frac{\partial \vec{v}}{\partial z}\right|^{-2} \tag{3.14}$$

with γ from Eq. 3.2 and γ_E from Eq. 3.7. According to Blackadar (1962), the mixing lengths l_m and l_h are given by

$$\begin{aligned} \frac{1}{l_m} &= \frac{1}{k\,z} + \frac{1}{\lambda_m} \\ \frac{1}{l_h} &= \frac{1}{k\,z} + \frac{1}{\lambda_h} \end{aligned} \tag{3.15}$$

with $\lambda_h = \lambda_m\sqrt{(3d)/2}$. The parameters λ_m and d are set to default values of $\lambda_m = 160\ m$ and $d = 5$.

3.2 Horizontal Diffusion

The horizontal diffusion parameterization based on the ideas of Laursen and Eliasen (1989), which, in the ECHAM-3 model (Roeckner et al. 1992), improves the results compared with a ∇^k horizontal diffusion. The diffusion is done in spectral space. The contribution to the tendency of a spectral prognostic variable X_n is

$$\frac{\partial X_n}{\partial t} = -k_X L_n X_n \tag{3.16}$$

where n defines the total wave number. L_n is a scale selective function of the total wave number and is chosen such that large scales are not damped while the damping gets stronger with increasing n:

$$L_n = \begin{cases} (n - n_\star)^\alpha & \text{for} \quad n > n_\star \\ \\ 0 & \text{for} \quad n \leq n_\star \end{cases} \tag{3.17}$$

where $n_\star$ is a cut-off wave number. The parameters $n_\star$ and α are set to default values of $n_\star = 15$ and $\alpha = 2$ similar to the ECHAM-3 model in T21 resolution (Roeckner et al. 1992). The diffusion coefficient k_X defines the timescale of the damping and depends on the variable. In the model, k_X is computed from prescribed damping time scales τ_X for the smallest waves. Default values of $\tau_D = 0.2$ days for divergence, $\tau_\xi = 1.1$ days for vorticity and $\tau_T = 15.6$ days for temperature and humidity are chosen, which are comparable with the respective values in the T21 ECHAM-3 model. In contrast to ECHAM-3, however, no level or velocity dependent additional damping is applied.

3.3 Radiation

3.3.1 Short Wave Radiation

The short wave radiation scheme bases on the ideas of Lacis and Hansen (1974) for the cloud free atmosphere. For the cloudy part, either constant albedos and transmissivities for high-middle- and low-level clouds may be prescribed or parameterizations following Stephens (1978) and Stephens et al. (1984) may be used.

The downward radiation flux density $F^{\downarrow SW}$ is assumed to be the product of the extraterristical solar flux density E_0 with different transmission factors for various processes:

$$F^{\downarrow SW} = \mu_0 \, E_0 \cdot \mathcal{T}_R \cdot \mathcal{T}_O \cdot \mathcal{T}_W \cdot \mathcal{T}_D \cdot \mathcal{T}_C \cdot \mathcal{R}_S \tag{3.18}$$

Here, μ_0 refers to the cosine of the solar zenith angle and the factor $\mathcal{R}_S$ incorporates different surface albedo values. The Indices of the transmissivities $\mathcal{T}$ denote Rayleigh scattering (R), ozone absorption (O), water vapor absorption (W) and absorption and scattering by aerosols (dust; D) and cloud droplets (C), respectively. E_0 and μ_0 are computed following Berger (1978a, 1978b). The algorithm used is valid to 1,000,000 years past or hence. The numeric to compute E_0 and μ_0 is adopted from the CCM3 climate model (Kiehl et al. 1996, coding by E. Kluzek 1997). The calculation accounts for earths orbital parameters and the earths distance to the sun, both depending on the year and the time of the year.

Following, for example, Stephens (1984) the solar spectral range is divided into two regions: (1) A visible and ultraviolet part for wavelengths $\lambda < 0.75$ μm with pure cloud scattering, ozone absorption and Rayleigh scattering, and without water vapor absorption. (2) A near infrared part for wavelengths $\lambda > 0.75$ μm with cloud scattering and absorption and with water vapor absorption. Absorption and scattering by aerosols is neglected in the present scheme. Dividing the total solar energy E_0 into the two spectral regions results in the fractions $E_1 = 0.517$ and $E_2 = 0.483$ for spectral ranges 1 and 2, respectively.

Clear sky

For the clear sky part of the atmospheric column parameterizations following Lacis and Hansen (1974) are used for Rayleigh scattering, ozone absorption and water vapor absorption.

Visible and ultraviolet spectral range ($\lambda < 0.75$ μm)

In the visible and ultraviolet range, Rayleigh scattering and ozone absorption are considered for the clear sky part. Rayleigh scattering is confined to the lowermost atmospheric layer. The transmissivity for this layer is given by

$$\mathcal{T}_{R1} = 1 - \frac{0.219}{1 + 0.816\mu_0} \tag{3.19}$$

for the direct beam, and

$$\mathcal{T}_{R1} = 1 - 0.144 \tag{3.20}$$

for the scattered part.

Ozone absorption is considered for the Chappuis band in the visible $\mathcal{A}^{vis}$ and for the ultraviolet range $\mathcal{A}^{uv}$. The total transmissivity due to ozone is given by

$$\mathcal{T}_{O1} = 1 - \mathcal{A}_O^{vis} - \mathcal{A}_O^{uv} \tag{3.21}$$

with

$$\mathcal{A}_O^{vis} = \frac{0.02118x}{1 + 0.042x + 0.000323x^2} \tag{3.22}$$

and

$$\mathcal{A}_O^{uv} = \frac{1.082x}{(1 + 138.6x)^{0.805}} + \frac{0.0658x}{1 + (103.6x)^3} \tag{3.23}$$

where the ozone amount traversed by the direct solar beam, x, is

$$x = M\ u_{O_3} \tag{3.24}$$

with u_{O_3} being the ozone amount [cm] in the vertical column above the considered layer, and M is the magnification factor after Rodgers (1967)

$$M = \frac{35}{(1224{\mu_0}^2 + 1)^{\frac{1}{2}}} \tag{3.25}$$

The ozone path traversed by diffuse radiation from below is

$$x^* = M\ u_{O_3} + \overline{M}\ (u_t - u_{O_3}) \tag{3.26}$$

where u_t is the total ozone amount above the main reflecting layer and $\overline{M}$=1.9 is the effective magnification factor for diffusive upward radiation.

Near infrared ($\lambda > 0.75\ \mu$m)

In the near infrared solar region absorption by water vapor is considered only. The transmissivity is given by

$$\mathcal{T}_{W2} = 1 - \frac{2.9y}{(1 + 141.5y)^{0.635} + 5.925y} \tag{3.27}$$

where y is the effective water vapor amount [cm] including an approximate correction for the pressure and temperature dependence of the absorption and the magnification factor M. For the direct solar beam, y is given by

$$y = \frac{M}{g} \int_0^p 0.1\ q \left(\frac{p}{p_0}\right) \left(\frac{T_0}{T}\right)^{\frac{1}{2}} dp \tag{3.28}$$

while for the reflected radiation reaching the layer from below, y is

$$y = \frac{M}{g} \int_0^{p_S} 0.1\ q \left(\frac{p}{p_0}\right) \left(\frac{T_0}{T}\right)^{\frac{1}{2}} dp + \frac{\beta_d}{g} \int_p^{p_S} 0.1\ q \left(\frac{p}{p_0}\right) \left(\frac{T_0}{T}\right)^{\frac{1}{2}} dp \tag{3.29}$$

with the acceleration of gravity g, the surface pressure p_S, a reference pressure $p_0 = 1000$ hPa, a reference temperature $T_0 = 273$ K, the specific humidity q [kg/kg] and the magnification factor for diffuse radiation $\beta_d = 1.66$.

Clouds

Two possibilities for the parameterization of the effect of clouds on the short wave radiative fluxes are implemented: (1) prescribed cloud properties and (2) a parameterization following Stephens (1978) and Stephens et al. (1984), which is the default setup.

Prescribed cloud properties

Radiative properties of clouds are prescribed depending on the cloud level. Albedos $\mathcal{R}_{C1}$ for cloud scattering in the visible spectral range ($\lambda < 0.75\ \mu$m), and albedos $\mathcal{R}_{C2}$ for cloud

scattering and absorptivities $\mathcal{A}_{C2}$ for cloud absorption in the near infrared part ($\lambda > 0.75$ μm) are defined for high, middle and low level clouds. The default values are listed in Table 3.1.

Cloud Level	Visible range $\mathcal{R}_{C1}$	Near infrared $\mathcal{R}_{C2}$	$\mathcal{A}_{C1}$
High	0.15	0.15	0.05
Middle	0.30	0.30	0.10
Low	0.60	0.60	0.20

Table 3.1: Prescribed cloud albedos $\mathcal{R}_C$ and absorptivities $\mathcal{A}_C$ for spectral range 1 and 2

Default: Parameterization according to Stephens (1978) and Stephens et al. (1984)

Following Stephens (1978) and Stephens et al. (1984) cloud parameters are derived from the cloud liquid water path W_L [g/m^2] and the cosine of the solar zenith angel μ_0. In the visible and ultraviolet range cloud scattering is present only while in the near infrared both, cloud scattering and absorption, are parameterized.

Visible and ultraviolet spectral range ($\lambda < 0.75$ μm)

For the cloud transmissivity $\mathcal{T}_{C1}$ Stephens parameterization for a non absorbing medium is applied:

$$\mathcal{T}_{C1} = 1 - \frac{\beta_1 \tau_{N1}/\mu_0}{1 + \beta_1 \tau_{N1}/\mu_0} = \frac{1}{1 + \beta_1 \tau_{N1}/\mu_0} \tag{3.30}$$

β_1 is the backscatter coefficient, which is available in tabular form. In order to avoid interpolation of tabular values the following interpolation formula is used

$$\beta_1 = f_{b1} \sqrt{\mu_0} \tag{3.31}$$

where the factor f_{b1} comprises a tuning opportunity for the cloud albedo and is set to a default value of 0.035.

τ_{N1} is an effective optical depth for which Stephens (1979) provided the interpolation formula

$$\tau_{N1} = 1.8336 \, (\log W_L)^{3.963} \tag{3.32}$$

which is approximated by

$$\tau_{N1} = 2 \, (\log W_L)^{3.9} \tag{3.33}$$

to be used also for the near infrared range (see below).

Near infrared ($\lambda > 0.75$ μm)

The transmissivity due to scattering and absorption of a cloud layer in the near infrared spectral range is

$$\mathcal{T}_{C2} = \frac{4u}{R} \tag{3.34}$$

where u is given by

$$u^2 = \frac{(1 - \tilde{\omega}_0 + 2 \, \beta_2 \, \tilde{\omega}_0)}{(1 - \tilde{\omega}_0)} \tag{3.35}$$

and R by

$$R = (u+1)^2 \exp(\tau_{eff}) - (u-1)^2 \exp(-\tau_{eff}) \tag{3.36}$$

with

$$\tau_{eff} = \frac{\tau_{N2}}{\mu_0}\sqrt{(1-\tilde{\omega}_0)(1-\tilde{\omega}_0+2\,\beta_2\,\tilde{\omega}_0)} \tag{3.37}$$

where the original formulation for the optical depth τ_{N2} by Stephens (1978)

$$\tau_{N2} = 2.2346\,(\log W_L)^{3.8034} \tag{3.38}$$

is, as for the visible range, approximated by

$$\tau_{N2} = 2\,(\log W_L)^{3.9} \tag{3.39}$$

Approximations for the table values of the back scattering coefficient β_2 and the single scattering albedo $\tilde{\omega}_0$ are

$$\beta_2 = \frac{f_{b2}\,\sqrt{\mu_0}}{\ln(3+0.1\,\tau_{N2})} \tag{3.40}$$

and

$$\tilde{\omega}_0 = 1 - f_{o2}\,\mu_0^2\,\ln(1000/\tau_{N2}) \tag{3.41}$$

where f_{b2} and f_{o2} provide a tuning of the cloud properties and are set to default values of f_{b2}=0.04 and f_{o2}=0.006.

The scattered flux is computed from the cloud albedo $\mathcal{R}_{C2}$ which is given by

$$\mathcal{R}_{C2} = [\exp(\tau_{eff}) - \exp(-\tau_{eff})]\,\frac{u^2-1}{R} \tag{3.42}$$

Vertical integration

For the vertical integration, the adding method is used (e.g. Lacis and Hansen 1974, Stephens 1984). The adding method calculates the reflection $\mathcal{R}_{ab}$ and transmission $\mathcal{T}_{ab}$ functions for a composite layer formed by combining two layers one (layer a) on top of the other (layer b). For the downward beam $\mathcal{R}_{ab}$ and $\mathcal{T}_{ab}$ are given by

$$\begin{aligned} \mathcal{R}_{ab} &= \mathcal{R}_a + \mathcal{T}_a\mathcal{R}_b\mathcal{T}_a^*/(1-\mathcal{R}_a^*\mathcal{R}_b) \\ \mathcal{T}_{ab} &= \mathcal{T}_a\mathcal{T}_b/(1-\mathcal{R}_a^*\mathcal{R}_b) \end{aligned} \tag{3.43}$$

where the denominator accounts for multiple reflections between the two layers. For illumination form below $\mathcal{R}_{ab}^*$ and $\mathcal{T}_{ab}^*$ are given by

$$\begin{aligned} \mathcal{R}_{ab}^* &= \mathcal{R}_b^* + \mathcal{T}_b^*\mathcal{R}_a^*\mathcal{T}_b/(1-\mathcal{R}_a^*\mathcal{R}_b) \\ \mathcal{T}_{ab}^* &= \mathcal{T}_a^*\mathcal{T}_b/(1-\mathcal{R}_a^*\mathcal{R}_b) \end{aligned} \tag{3.44}$$

The following four steps are carried out to obtain the radiative upward and downward fluxes at the boundary between two layers from which the total flux and the absorption (heating rates) are calculated:

1) $\mathcal{R}_l$ and $\mathcal{T}_l$, $l = 1, L$ are computed for each layer and both spectral regions according to the parameterizations.

2) The layers are added, going down, to obtain $\mathcal{R}_{1,l}$ and $\mathcal{T}_{1,l}$ for $L = 2, L+1$ and $\mathcal{R}^*_{1,l}$ and $\mathcal{T}^*_{1,l}$ for $L = 2, L$.

3) Layers are added one at the time, going up, to obtain $\mathcal{R}_{L+1-l,L+1}$, $l = 1, L-1$ starting with the ground layer, $\mathcal{R}_{L+1} = \mathcal{R}_S$ which is the surface albedo and $\mathcal{T}_{L+1}$=0.

4) The upward $F_l^{\uparrow SW}$ and downward $F_l^{\downarrow SW}$ short wave radiative fluxes at the interface of layer $(1, l)$ and layer (l+1,L+1) are determined from

$$\begin{aligned} F_l^{\uparrow SW} &= \mathcal{T}_{1,l}\, \mathcal{R}_{l+1,L+1}/(1 - \mathcal{R}^*_{1,l}\, \mathcal{R}_{l+1,L+1}) \\ F_l^{\downarrow SW} &= \mathcal{T}_{1,l}/(1 - \mathcal{R}^*_{1,l}\, \mathcal{R}_{l+1,L+1}) \end{aligned} \tag{3.45}$$

The net downward flux at level l, $F_l^{\updownarrow SW}$, is given by

$$F_l^{\updownarrow SW} = F_l^{\downarrow SW} - F_l^{\uparrow SW} \tag{3.46}$$

Finally, the temperature tendency for the layer between l and $l+1$ is computed:

$$\frac{\Delta T_{l+\frac{1}{2}}}{2\Delta t} = -\frac{g}{c_p\, p_S} \frac{F_{l+1}^{\updownarrow SW} - F_l^{\updownarrow SW}}{\Delta\sigma} \tag{3.47}$$

3.3.2 Long Wave Radiation

Clear sky

For the clear sky long wave radiation, the broad band emissivity method is employed (see, for example, Manabe and Möller 1961, Rodgers 1967, Sasamori 1968, Katayama 1972, Boer et al. 1984). Using the broad band transmissivities $\mathcal{T}_{(z,z')}$ between level z and level z', the upward and downward fluxes at level z, $F^{\uparrow LW}(z)$ and $F^{\downarrow LW}(z)$, are

$$\begin{aligned} F^{\uparrow LW}(z) &= \mathcal{A}_S\, B(T_S)\mathcal{T}_{(z,0)} + \int_0^z B(T')\frac{\partial \mathcal{T}_{(z,z')}}{\partial z'}dz' \\ F^{\downarrow LW}(z) &= \int_\infty^z B(T')\frac{\partial \mathcal{T}_{(z,z')}}{\partial z'}dz' \end{aligned} \tag{3.48}$$

where $B(T)$ denotes the black body flux ($B(T) = \sigma_{SB}T^4$) and $\mathcal{A}_S$ is the surface emissivity. The effect of water vapor, carbon dioxide and ozone is included in the calculations of the transmissivities $\mathcal{T}$ (with $\mathcal{T} = 1 - \mathcal{A}$, where $\mathcal{A}$ is the absoroptivity/emissivity). The transmissivities for water vapor $\mathcal{T}_{H_2O}$, carbon dioxide $\mathcal{T}_{CO_2}$ and ozone $\mathcal{T}_{O_3}$ are taken from Sasamori (1968):

$$\mathcal{T}_{H_2O} = 1 - 0.846\,(u_{H_2O} + 3.59\cdot 10^{-5})^{0.243} - 6.90\cdot 10^{-2}$$

for $u_{H_2O} < 0.01$ g, and

$$\mathcal{T}_{H_2O} = 1 - 0.240\log(u_{H_2O} + 0.010) + 0.622$$

else.

$$\mathcal{T}_{CO_2} = 1 - 0.0825\, u_{CO_2}^{0.456} \tag{3.49}$$

for $u_{CO_2} \le 0.5$ cm, and

$$\mathcal{T}_{CO_2} = 1 - 0.0461\log(u_{CO_2}) + 0.074$$

else.

$$\mathcal{T}_{O_3} = 1 - 0.0122\log(u_{O_3} + 6.5\cdot 10^{-4}) + 0.0385$$

where u_{H_2O}, u_{CO_2} and u_{O_3} are the effective amounts of water vapor, carbon dioxide and ozone, respectively, which are obtained from:

$$u(p,p') = \frac{f}{g}\int_p^{p'} q_X\left(\frac{p''}{p_0}\right)dp'' \tag{3.50}$$

where q_X denotes the mixing ratios [kg/kg] of water vapor, carbon dioxide and ozone, respectively, g is the gravitational acceleration, p is pressure and $p_0 = 1000$ hPa is the reference pressure. The factor f is used to transfer the units to g/cm^2 for u_{H_2O} and cm-STP for u_{CO_2} and cm-STP for u_{O_3}, which are used in Eq. 3.49.

To account for the overlap between the water vapor and the carbon dioxide bands near 15 μm, the CO_2 absorption is corrected by a H_2O transmission at 15 μm, $\mathcal{T}_{H_2O}^{15\mu m}$, with $\mathcal{T}_{H_2O}^{15\mu m}$ given by

$$\mathcal{T}_{H_2O}^{15\mu m} = 1.33 - 0.832\,(u_{H_2O} + 0.0286)^{0.26} \tag{3.51}$$

Clouds

Clouds can be either treated as gray bodies with a prescribed cloud flux emissivity (grayness) or the cloud flux emissivity is obtained from the cloud liquid water contend. If the cloud flux emissivity (grayness) $\mathcal{A}^{cl}$ is externally prescribed, the value is attributed to each cloud layer. Otherwise, which is the default, $\mathcal{A}^{cl}$ is calculated from the cloud liquid water (e.g. Stephens 1984)

$$\mathcal{A}^{cl} = 1. - \exp\left(-\beta_d\, k^{cl}\, W_L\right) \tag{3.52}$$

where $\beta_d = 1.66$ is the diffusivity factor, k^{cl} is the mass absorption coefficent (with is set to a default value of 0.1 m^2/g (Slingo and Slingo 1991)) and W_L is the cloud liquid water path.

For a single layer between z and z' with fractional cloud cover cc, the total transmissivity $\mathcal{T}^*_{(z,z')}$ is given by

$$\mathcal{T}^*_{(z,z')} = \mathcal{T}_{(z,z')}\,(1 - cc\,\mathcal{A}^{cl}) \tag{3.53}$$

where $\mathcal{T}_{(z,z')}$ is the clear sky transmissivity. When there is more than one cloud layer with fractional cover, random overlapping of the clouds is assumed and $\mathcal{T}^*_{(z,z')}$ becomes

$$\mathcal{T}^*_{(z,z')} = \mathcal{T}_{(z,z')} \prod_j (1 - cc_j\,\mathcal{A}^{cl}_j) \tag{3.54}$$

where the subscript j denotes the cloud layers.

Vertical discretization

To compute the temperature tendency for a model layer resulting form the divergence of the radiative fluxes, the vertical discretization scheme of Chou et al. (2002) is used. The upward and downward fluxes, $F_l^{\uparrow LW}$ and $F_l^{\downarrow LW}$, at level l, which is the interface between two model layers, are computed from

$$\begin{aligned} F_l^{\uparrow LW} &= \sum_{l'=l}^{L} B_{l'+\frac{1}{2}}[\mathcal{T}^*_{(l,l')} - \mathcal{T}^*_{(l'+1,l)}] \qquad l = 1, \cdots, L \\ &\quad + \mathcal{T}^*_{(l,L+1)}\; F_{L+1}^{\uparrow LW} \end{aligned} \tag{3.55}$$

$$F_l^{\downarrow LW} = \sum_{l'=1}^{l-1} B_{l'+\frac{1}{2}}[\mathcal{T}^*_{(l'+1,l)} - \mathcal{T}^*_{(l',l)}] \qquad l = 2, \cdots, L+1$$

where $\mathcal{T}^*_{(l,l')}$ denotes the transmissivity of the layer from level l to level l' (see above) and $B_{l+\frac{1}{2}}$ is the black body flux for level $l + \frac{1}{2}$. The downward flux at the top of the atmosphere, $F_0^{\downarrow LW}$, and the upward flux at the surface ,$F_{L+1}^{\uparrow LW}$, are given by

$$\begin{aligned} F_0^{\downarrow LW} &= 0 \\ F_{L+1}^{\uparrow LW} &= \mathcal{A}_S\; B(T_S) + (1 - \mathcal{A}_S)\; F_{L+1}^{\downarrow LW} \end{aligned} \tag{3.56}$$

where $\mathcal{A}_S$ denotes the surface emissivity and T_S is the surface temperature. Note, that for a more convenient discription of the scheme, $l + \frac{1}{2}$ denotes a so called full level, where the

temperatures are defined. This may be in contrast to the convention in most of the other sections where a full level is indicated by l.

Eqs. 3.55 can be rearranged to give

$$\begin{aligned} F_l^{\uparrow LW} &= B_{l+\frac{1}{2}} + \sum_{l'=l+1}^{L+1} \mathcal{T}^*_{(l',l)} \left[B_{l'+\frac{1}{2}} - B_{l'-\frac{1}{2}}\right] \qquad l = 1, \cdots, L \\ &\quad + \mathcal{T}^*_{(l,L+1)} \left(1 - \mathcal{A}_S\right) F_{L+1}^{\downarrow LW} \end{aligned} \tag{3.57}$$

$$F_{l'}^{\downarrow LW} = B_{l'-\frac{1}{2}} - \sum_{l=1}^{l'-1} \mathcal{T}^*_{(l',l)} \left[B_{l+\frac{1}{2}} - B_{l-\frac{1}{2}}\right] \qquad l' = 2, \cdots, L+1$$

with the boundary conditions

$$\begin{aligned} B_{L+\frac{3}{2}} &= \mathcal{A}_S \, B(T_S) \\ B_{\frac{1}{2}} &= 0 \end{aligned} \tag{3.58}$$

The net downward flux at level l, $F_l^{\updownarrow LW}$, is given by

$$F_l^{\updownarrow LW} = F_l^{\downarrow LW} - F_l^{\uparrow LW} \tag{3.59}$$

Finally, the temperature tendency for the layer between l and $l+1$ is computed:

$$\frac{\Delta T_{l+\frac{1}{2}}}{2\Delta t} = -\frac{g}{c_p \, p_S} \frac{F_{l+1}^{\updownarrow LW} - F_l^{\updownarrow LW}}{\Delta\sigma} \tag{3.60}$$

Emission of a layer

As pointed out by Chou et al. (2002), the difference between the upward and downward emission of a layer will be large, if the layer is rather opaque and the temperature range across the layer is large. This, in particular, holds for coarse vertical resolution as in the default version of the model. Therefore, the upward and the downward emission of a layer is computed separately following the ideas of Chou et al. (2002):

The contribution of the upward flux at level p from the adjecant layer below can be written as

$$\Delta F^{\uparrow LW}(p) = -\int_p^{p+\Delta p} B(p') \, \frac{\partial \mathcal{T}_{(p,p')}}{\partial p'} \, dp' = B^u \left(1 - \mathcal{T}_{(p+\Delta p,p)}\right) \tag{3.61}$$

where Δp is the thickness of the adjacent layer, B^u is the effective Planck flux for the adjacent layer, and $\mathcal{T}_{(p+\Delta p,p)}$ is the flux transmittance between p and $p+\Delta p$. Assuming that the Planck function varies linearly with pressure and the transmittance decreases exponentially with pressure away from p it follows

$$B(p') = B(p) + \frac{(B(p) - B(p+\Delta p))(p'-p)}{\Delta p} \tag{3.62}$$

and

$$\mathcal{T}_{(p,p')} = \exp\left(-c \, (p'-p)\right) \tag{3.63}$$

with c ia a constant. From Eq. 3.61 the effective Planck flux for the adjacent layer B^u is

$$B^u = \frac{B(p) - B(p+\Delta p)\ \mathcal{T}_{(p+\Delta p,p)}}{1-\mathcal{T}_{(p+\Delta p,p)}} + \frac{B(p)-B(p+\Delta p)}{\ln(\mathcal{T}_{(p+\Delta p,p)})} \tag{3.64}$$

Similarly, for the downward flux at the lower boundary of the layer, the effective Planck function of the layer B^d is

$$B^d = \frac{B(p+\Delta p) - B(p)\ \mathcal{T}_{(p+\Delta p,p)}}{1-\mathcal{T}_{(p+\Delta p,p)}} + \frac{B(p+\Delta p)-B(p)}{\ln(\mathcal{T}_{(p+\Delta p,p)})} \tag{3.65}$$

Replacing the respective Planck functions in Eqs. 3.57 by B^u and B^d results in

$$\begin{aligned} F_l^{\uparrow LW} &= B^u_{l+\frac{1}{2}} + \sum_{l'=l+1}^{L+1} \mathcal{T}^*_{(l',l)} \left[B^u_{l'+\frac{1}{2}} - B^u_{l'-\frac{1}{2}}\right] \qquad l = 1,\cdots,L \\ &\quad + \mathcal{T}^*_{(l,L+1)}\,(1-\mathcal{A}_S)\ F^{\downarrow LW}_{L+1} \end{aligned} \tag{3.66}$$

$$F_{l'}^{\downarrow LW} = B^d_{l'-\frac{1}{2}} - \sum_{l=1}^{l'-1} \mathcal{T}^*_{(l',l)} \left[B^d_{l+\frac{1}{2}} - B^d_{l-\frac{1}{2}}\right] \qquad l' = 2,\cdots,L+1$$

where

$$\begin{aligned} B^d_{l'-\frac{1}{2}} &= \frac{B_{l'} - B_{l'-1}\ \mathcal{T}_{(l',l'-1)}}{1-\mathcal{T}_{(l',l'-1)}} + \frac{B_{l'}-B_{l'-1}}{\ln(\mathcal{T}_{(l',l'-1)})} \\ B^u_{l'-\frac{1}{2}} &= (B_{l'}+B_{l'-1}) - B^d_{l'-\frac{1}{2}} \end{aligned} \tag{3.67}$$

For the calculation of the effective Plank function, the mean transmissivity for a layer partially filled with clouds is given by

$$\mathcal{T}_{(l',l'-1)} = f_{\mathcal{T}}\ \mathcal{T}^{cs}_{(l',l'-1)}\ (1 - cc_{(l',l'-1)}\mathcal{A}^{cl}_{(l',l'-1)}) \tag{3.68}$$

with the cloud emissivity $\mathcal{A}^{cl}$ and the clear sky transmissivity $\mathcal{T}^{cs}$ being defined above, and the factor $f_{\mathcal{T}}$ provides a tuning opportunity.

When a model layer spans a region where the temperature lapse rate changes signs, the linearity of B with respect to p can not longer be assumed and B^d and B^u are simply computed from

$$B^u_{l+\frac{1}{2}} = B^d_{l-\frac{1}{2}} = 0.5\ B_{l+\frac{1}{2}} + 0.25\ (B_l + B_{l'}) \tag{3.69}$$

3.3.3 Ozone

Ozone concentration is prescribed. Either a three dimensional ozone distribution can be externally provided or an idealized annual cycle of ozone concentration can be used. The idealized distribution bases on the analytic ozone distribution of Green (1964):

$$u_{O_3}(h) = \frac{a + a\ \exp(-b/c)}{1+\exp((h-b)/c)} \tag{3.70}$$

where $u_{O_3}(h)$ is the ozone amount [cm-STP] in a vertical column above the altitude h, a is the total ozone amount in a vertical column above the ground, b the altitude at which the ozone concentration has its maximum. While for $a = 0.4$ cm, $b = 20$ km and $c = 5$ km this distribution fits close to the mid-latitude winter ozone distribution, an annual cycle and a latitudinal dependence is introduced by varying a with time and latitude.

3.3.4 Additional Newtonian cooling

For the standard setup with a vertical resolution of five equally spaced sigma-levels, the model produces a strong bias in the stratospheric (uppermost level) temperatures. This may be attributed to the insufficient representation of the stratosphere and its radiative and dynamical processes. The bias also effects the tropospheric circulation leading, for example, to a misplacement of the dominant pressure centers. To enable the simulation of a more realistic tropospheric climate, a Newtonian cooling can be applied to the uppermost level. Using this method, the model temperature T is relaxed towards a externally given distribution of the temperature T_{NC} which results in additional temperature tendencies $\dot{T}$ for the uppermost model level of

$$\dot{T} = \frac{T_{NC} - T}{\tau_{NC}} \tag{3.71}$$

where τ_{NC} is the time scale of the relaxation, which has a default value of ten days.

3.4 Moist Processes and Dry Convection

3.4.1 Correction of Negative Humidity

Local negative values of specific humidity are an artifact of spectral models. In the model, a simple procedure corrects these negative values by conserving the global amount of water. The correction of negative moisture is performed at the beginning of the grid-point parameterization scheme. A negative value of specific humidity is reset to zero. Accumulation of all corrections defines a correction factor. A hierarchical scheme of three steps is used. First, the correction is done within an atmospheric column only. If there are atmospheric columns without sufficient moisture, a second correction step is done using all grid points of the respective latitude. Finally, if there is still negative humidity remaining, a global correction is performed.

3.4.2 Saturation Specific Humidity

For parameterizations of moist processes like cumulus convection and large scale condensation the computation of the saturation specific humidity $q_{sat}(T)$ and its derivative with respect to temperature $dq_{sat}(T)/dT$ is needed at several places. In the model, the Tetens formula (Lowe 1977) is used to calculate the saturation pressure $e_{sat}(T)$ and its derivative with respect to temperature $de_{sat}(T)/dT$:

$$\begin{aligned} e_{sat}(T) &= a_1 \exp\left(a_2 \frac{T - T_0}{T - a_3}\right) \\ \frac{de_{sat}(T)}{dT} &= \frac{a_2 \, (T_0 - a_3)}{(T - a_3)^2} \, e_{sat}(T) \end{aligned} \tag{3.72}$$

with the constants $a_1 = 610.78$, $a_2 = 17.2693882$, $a_3 = 35.86$ and $T_0 = 273.16$. The saturation specific humidity $q_{sat}(T)$ and its derivative $dq_{sat}(T)/dT$ are given by

$$\begin{aligned} q_{sat}(T) &= \frac{\epsilon \, e_{sat}(T)}{p - (1 - \epsilon) \, e_{sat}(T)} \\ \frac{dq_{sat}(T)}{dT} &= \frac{p \, q_{sat}(T)}{p - (1 - \epsilon) \, e_{sat}(T)} \frac{de_{sat}(T)}{dT} \end{aligned} \tag{3.73}$$

where p is the pressure and ϵ is the ration of the gas constants for dry air R_d and water vapor R_v ($\epsilon = R_d/R_v$).

3.4.3 Cumulus Convection

The cumulus convection is parameterized by a Kuo-type convection scheme (Kuo 1965, 1974) with some modifications to the original Kuo-scheme. The Kuo-scheme considers the effect of cumulus convection on the large scale flow applying the following assumptions. Cumulus clouds are forced by mean low level convergence in regions of conditionally unstable stratification. The production of cloud air is proportional to the net amount of moisture convergence into one grid box column plus the moisture supply by surface evaporation. In a modification to the original scheme, the implemented scheme also considers clouds which originate at upper levels where moisture convergence is observed. This type of cloud may occur in mid-latitude frontal regions. Therefore, only the moisture contribution which takes place in the layer between the lifting level and the top of the cloud is used instead of the whole column. Thus, the total moisture supply I in a period $2\Delta t$ is given by

$$I = \frac{2\Delta t\, p_S}{g} \int\limits_{\sigma_{Top}}^{\sigma_{Lift}} A_q \, d\sigma \tag{3.74}$$

where A_q is the moisture convergence plus the surface evaporation if the lifting level σ_{Lift} is the lowermost model level. σ_{Top} is the cloud top level, p_S is the surface pressure and g is the gravitational acceleration. Lifting level, cloud base and cloud top are determined as follows. Starting form the lowermost level, the first level with positive moisture supply A_q is considered as a lifting level. If the lowermost level L is considered to be a lifting level and the surface layer is dry adiabatic unstable ($\theta_S > \theta_L$ where θ denotes the potential temperature), the convection starts from the surface. Air from the lifting level $(l+1)$ is lifted dry adiabatically up to the next level (l) by keeping its specific humidity. A cloud base is assumed to coincide with level $l + \frac{1}{2}$ if the air is saturated at l. Above the cloud base the air is lifted moist adiabatically. Distribution of temperature T_{cl} and of moisture q_{cl} in the cloud is found by first lifting the air dry adiabatically

$$\begin{aligned} (T_{cl})_l^{Ad} &= (T_{cl})_{l+1} \left(\frac{\sigma_l}{\sigma_{l+1}} \right)^{\frac{R_d}{c_{pd}}} \\ (q_{cl})_l^{Ad} &= (q_{cl})_{l+1} \end{aligned} \tag{3.75}$$

and then by correcting temperature and moisture values due to the condensation of water vapor

$$\begin{aligned} (T_{cl})_l &= (T_{cl})_l^{Ad} + \frac{L}{c_p} \frac{(q_{cl})_l^{Ad} - q_{sat}[(T_{cl})_l^{Ad}]}{1 + \frac{L}{c_p} \frac{dq_{sat}[(T_{cl})_l^{Ad}]}{dT}} \\ (q_{cl})_l &= (q_{cl})_l^{Ad} - \frac{(q_{cl})_l^{Ad} - q_{sat}[(T_{cl})_l^{Ad}]}{1 + \frac{L}{c_p} \frac{dq_{sat}[(T_{cl})_l^{Ad}]}{dT}} \end{aligned} \tag{3.76}$$

where the suturation specific humidity q_{sat} and its derivative with respect to temperature dq_{sat}/dT are computed from Eqs. 3.73. L is either the latent heat of vapourisation L_v or the latent heat of sublimation L_s depending on the temperature. c_p is the specific heat for moist air at constant pressure ($c_p = c_{pd}\,[1 + (c_{pv}/c_{pd} - 1)\,q]$ where c_{pd} and c_{pv} are the specific heats at constant pressure for dry air and water vapor, respectively) and R_d in Eq. 3.75 is the gas constant for dry air. For reasons of accuracy the calculation (3.76) is repeated once where $(T_{cl})^{Ad}$ and $(q_{cl})^{Ad}$ are now replaced by the results of the first iteration.

Cumulus clouds are assumed to exist only if the environmental air with temperature T_e and moisture q_e is unstable stratified with regard to the rising cloud parcel:

$$(T_{cl})_l > (T_e)_l \tag{3.77}$$

The top of the cloud σ_{Top} is then defined as

$$\sigma_{Top} = \sigma_{l+\frac{1}{2}} \text{ if } \begin{cases} (T_{cl})_l \leq (T_e)_l & \text{and} \\ (T_{cl})_{l+1} > (T_e)_{l+1} \end{cases} \tag{3.78}$$

Cumulus clouds do exist only if the net moisture accession I as given by Eq. 3.74 is positive. Once this final check has been done, the heating and moistening of the environmental air and the convective rain are computed.

In the model either the original scheme proposed by Kuo (1968) or the modified scheme with the parameter β (Kuo 1974) can be chosen, where β determines the partitioning of heating and moistening of the environmental air. In the scheme without β the surplus P of total energy of the cloud against the environmental air is given by

$$P = \frac{p_s}{g} \int_{\sigma_{Top}}^{\sigma_{Base}} (c_p (T_{cl} - T_e) + L (q_{sat}(T_e) - q_e)) d\sigma \tag{3.79}$$

The clouds produced dissolve instantaneously by artificial mixing with the environmental air, whereby the environment is heated and moistened by

$$\begin{aligned} (\Delta T)^{cl} &= a (T_{cl} - T_e) \\ (\Delta q)^{cl} &= a (q_{sat}(T_e) - q_e) \end{aligned} \tag{3.80}$$

where a is the fractional cloud area being produced by the moisture supply:

$$a = L \frac{I}{P} \tag{3.81}$$

In the scheme with β the fraction 1-β of the moisture is condensed, while the remaining fraction β is stored in the atmosphere. The parameter β depends on the mean relative humidity and, in the present scheme, is given by

$$\beta = \left(1 - \frac{1}{\sigma_{Base} - \sigma_{Top}} \int_{\sigma_{Top}}^{\sigma_{Base}} \frac{q_e}{q_{sat}(T_e)} d\sigma \right)^3 \tag{3.82}$$

Instead of Eq. 3.80, the temperature and moisture tendencies are now

$$\begin{aligned} (\Delta T)^{cl} &= a_T (T_{cl} - T_e) \\ (\Delta q)^{cl} &= a_q (q_{sat}(T_e) - q_e) \end{aligned} \tag{3.83}$$

where a_T and a_q are given by

$$\begin{aligned} a_T &= \frac{(1 - \beta) L I}{c_p \frac{p_S}{g} \int_{\sigma_{Top}}^{\sigma_{Base}} (T_{cl} - T_e) d\sigma} \\ a_q &= \frac{\beta I}{\frac{p_S}{g} \int_{\sigma_{Top}}^{\sigma_{Base}} (q_{sat}(T_e) - q_e) d\sigma} \end{aligned} \tag{3.84}$$

The final tendencies for moisture $\partial q/\partial t$ and temperature $\partial T/\partial t$ which enter the diabatic leap frog time step are given by

$$\begin{aligned} \frac{\partial q}{\partial t} &= \frac{(\Delta q)^{cl}}{2\Delta t} - \delta^{cl} A_q \\ \frac{\partial T}{\partial t} &= \frac{(\Delta T)^{cl}}{2\Delta t} \end{aligned} \tag{3.85}$$

where δ^{cl} is specified by

$$\delta^{cl} = \begin{cases} 1 & \text{if } \sigma_{Top} \leq \sigma \leq \sigma_{Lift} \\ \\ 0 & \text{otherwise} \end{cases} \tag{3.86}$$

and $2\Delta t$ is the leap frog time step of the model. The convective precipitation rate P_c [m/s] of each cloud layer is

$$P_c = \frac{c_p\,\Delta p}{L\,g\,\rho_{H_2O}} \frac{(\Delta T)^{cl}}{2\Delta t} \tag{3.87}$$

where Δp is the pressure thickness of the layer and ρ_{H_2O} is the density of water. $(\Delta T)^{cl}$ is computed from Eq. 3.80 or Eq. 3.83, respectively.

3.4.4 Large Scale Precipitation

Large scale condensation occurs if the air is supersaturated ($q > q_{sat}(T)$). Condensed water falls out instantaneously as precipitation. No storage of water in clouds is considered. An iterative procedure is used to compute final values (T^*, q^*) starting from the supersaturated state (T, q):

$$\begin{aligned} T^* &= T + \frac{L}{c_p} \frac{q - q_{sat}(T)}{1 + \frac{L}{c_p} \frac{dq_{sat}(T)}{dT}} \\ \\ q^* &= q - \frac{q - q_{sat}(T)}{1 + \frac{L}{c_p} \frac{dq_{sat}(T)}{dT}} \end{aligned} \tag{3.88}$$

where the suturation specific humidity q_{sat} and its derivative with respect to temperature dq_{sat}/dT are computed from Eqs. 3.73. L is either the latent heat of vapourisation or the latent heat of sublimation depending on the temperature. c_p is the specific heat for moist air at constant pressure ($c_p = c_{pd}\,[1 + (c_{pv}/c_{pd} - 1)\,q]$ where c_{pd} and c_{pv} are the specific heats at constant pressure for dry air and water vapor, respectively). This calculation is repeated once using (T^*, q^*) as the new initial state. Finally, The temperature and moisture tendencies and the precipitation rate P_l [m/s] are computed:

$$\begin{aligned} \frac{\partial T}{\partial t} &= \frac{T^* - T}{2\Delta t} \\ \\ \frac{\partial q}{\partial t} &= \frac{q^* - q}{2\Delta t} \\ \\ P_l &= \frac{p_S\,\Delta\sigma}{g\,\rho_{H_2O}} \frac{(q - q^*)}{2\Delta t} \end{aligned} \tag{3.89}$$

where p_S is the surface pressure, ρ_{H_2O} is the density of water, $\Delta\sigma$ is the layer thickness and $2\Delta t$ is the leap frog time step of the model.

3.4.5 Cloud Formation

Cloud cover and cloud liquid water content are diagnostic quantities. The fractional cloud cover of a grid box, cc, is parameterized following the ideas of Slingo and Slingo (1991) using the relative humidity for the stratiform cloud amount cc_s and the convective precipitation rate P_c [mm/d] for the convective cloud amount cc_c. The latter is given by

$$cc_c = 0.245 + 0.125 \ln (P_c) \tag{3.90}$$

where $0.05 \leq cc_c \leq 0.8$.

Before computing the amount of stratiform clouds, the relative humidity rh is multiplied by $(1 - cc_c)$ to account for the fraction of the grid box covered by convective clouds. If $cc_c \geq 0.3$ and the cloud top is higher than $\sigma = 0.4$ ($\sigma = p/p_S$), anvil cirrus is present and the cloud amount is

$$cc_s = 2 \, (cc_c - 0.3) \tag{3.91}$$

High-, middle- and low-level stratiform cloud amounts are computed from

$$cc_s = f_\omega \left(\frac{rh - rh_c}{1 - rh_c} \right)^2 \tag{3.92}$$

where rh_c is a level depending critical relative humidity. Optionally, a restriction of low-level stratiform cloud amount due to subsidence can by introduced by the factor f_ω where f_ω is depends on the vertical velocity ω. In the default version, $f_\omega = 1$.

Cloud liquid water content q_{H_2O} [kg/kg] is computed according to Kiehl et al. (1996):

$$q_{H_2O} = \frac{q^0_{H_2O}}{\rho} \exp (-z/h_l) \tag{3.93}$$

where the reference value $q^0_{H_2O}$ is $0.21 \cdot 10^{-3}$ kg/m^3, ρ is the air density, z is the height and the local cloud water scale height h_l [m] is given by vertically integrated water vapor (precipitable water)

$$h_l = 700 \ln \left(1 + \frac{1}{g} \int_0^{p_s} q dp \right) \tag{3.94}$$

3.4.6 Evaporation of Precipitation and Snow Fall

Possible phase changes of convective or large scale precipitation within the atmosphere or the condensational growth of cloud droplets are not considered in the model. However, a distinction between rain and snow fall at the surface is made. If the temperature of the lowermost level exceeds the freezing point ($T > 273.16$ K), convective and large scale precipitation is assumed to be rain, otherwise all precipitation fall out as snow.

3.4.7 Dry Convective Adjustment

Dry convective adjustment is performed for layers which are dry adiabatically unstable, e.g. $\partial\theta/\partial p > 0$ where θ denotes the potential temperature. The adjustment is done so that the total sensible heat of the respective column is conserved. Wherever dry convection occurs, it is assumed that the moisture is completely mixed by the convective process as well. The adjustment is done iteratively. The atmospheric column is scanned for unstable regions. A new neutral stable state for the unstable region is computed which consists of a potential temperature θ_N and specific humidity q_N:

$$\begin{aligned} \theta_N &= \frac{\sum_{l=l_1}^{l_2} T_l \, \Delta\sigma_l}{\sum_{l=l_1}^{l_2} \sigma_l^\kappa \, \Delta\sigma_l} \\ q_N &= \frac{\sum_{l=l_1}^{l_2} q_l \, \Delta\sigma_l}{\sum_{l=l_1}^{l_2} \Delta\sigma_l} \end{aligned} \tag{3.95}$$

where l_1 and l_2 define the unstable region, $\sigma = (p/p_S)$ is the vertical coordinate, T and q are temperature and specific humidity, respectively, and κ is R_d/c_{pd} where R_d and c_{pd} are the gas constant and the specific heat for dry air, respectively.

The procedure is repeated starting from the new potential temperatures und moistures until all unstable regions are removed. The temperature and moisture tendencies which enter the diabatic time steps are then computed from the final θ_N and q_N

$$\begin{aligned} \frac{T_l^{t+\Delta t} - T_l^{t-\Delta t}}{2\Delta t} &= \frac{\theta_N \, \sigma_l^\kappa - T_l^{t-\Delta t}}{2\Delta t} \\ \frac{q_l^{t+\Delta t} - q_l^{t-\Delta t}}{2\Delta t} &= \frac{q_N - q_l^{t-\Delta t}}{2\Delta t} \end{aligned} \tag{3.96}$$

3.5 Land Surface and Soil

The parameterizations for the land surface and the soil include the calculation of temperatures for the surface and the soil, a soil hydrology and a river transport scheme. In addition, surface properties like the albedo, the roughness length or the evaporation efficiency are provided. As, at the moment, coupling to an extra glacier module is not available, glaciers are treated like other land points, but with surface and soil properties appropriate for ice. Optionally, A simple biome model can be used (see AXEL).

3.5.1 Temperatures

The surface temperature T_S is computed from the linearized energy balance of the uppermost z_{top} meters of the ground:

$$c_{top}\ z_{top}\ \frac{\Delta T_S}{\Delta t} = F_S - G + \Delta T_S\ \frac{\partial (Q_a - F_g)}{\partial T_S} - F_m \tag{3.97}$$

z_{top} is a prescribed parameter and set to a default value of $z_{top} = 0.20$ m. Q_a denotes the total heat flux from the atmosphere, which consists of the sensible heat flux, the latent heat flux, the net short wave radiation and the net long wave radiation. Q_g is the flux into the deep soil. Q_a and Q_g are defined positive downwards. Q_m is the snow melt heat flux and c_{top} is the volumetric heat capacity. Depending on the snow pack, z_{top} can partly or totally consist of snow or soil solids: $z_{top} = z_{snow} + z_{soil}$. Thus, the heat capacity c_{top} is a combination of snow and soil heat capacities:

$$c_{top} = \frac{c_{snow}\ c_{soil}\ z_{top}}{c_{snow}\ z_{soil} + c_{soil}\ z_{snow}} \tag{3.98}$$

The default value of c_{snow} is $0.6897 \cdot 10^6$ J/(kg K) using a snow density of 330 kg/m^3. c_{soil} is set to a default value of $2.07 \cdot 10^6$ J/(kg K) for glaciers and to a value of $2.4 \cdot 10^6$ J/(kgK) otherweise.

Below z_{top} the soil column is discretized into N layers with thickness Δz_i, where layer 1 is the uppermost of the soil layers. The default values for the model are $N = 5$ and $\Delta z =$ (0.4 m, 0.8 m, 1.6 m, 3.2 m, 6.4 m). The heat flux into layer 1, Q_g, is given by

$$Q_g = \frac{2k_1}{\Delta z_1}(T_S - T_1) \tag{3.99}$$

where k_1 and T_1 are the thermal conductivity and the temperature. If the snow depth is greater than z_{top}, the thermal properties of snow are blended with the first soil layer to create a snow/soil layer with thickness $z_{snow} - z_{top} + \Delta z_1$. The thermal conductivity k_1 and heat capacity c_1 of a snow/soil layer are

$$\begin{aligned} k_1 &= \frac{k_{snow}\ k_{soil}\ (\Delta z_1 + z_{snow} - z_{top})}{k_{snow}\ \Delta z_1 + k_{soil}\ (z_{snow} - z_{top})} \\ c_1 &= \frac{c_{snow}\ c_{soil}\ (\Delta z_1 + z_{snow} - z_{top})}{c_{snow}\ \Delta z_1 + c_{soil}\ (z_{snow} - z_{top})} \end{aligned} \tag{3.100}$$

with default values of $k_{snow} = 0.31$ W/(m K), $k_{soil} = 2.03$ W/(m K) for glaciers and $k_{soil} = 7$ W/(m K) otherweise.

After the surface temperature T_S has been calculated from Eq. 3.97, snow melts when T_S is greater than the freezing temperature T_{melt}. In this case, T_S is set to T_{melt} and a new atmospheric heat flux $Q_a(T_{melt})$ is calculated from Q_a and $\partial Q_a/\partial T_S$. If the energy inbalance

is positive ($Q_a(T_{melt}) > c_{top}\ z_{top}\ (T_{melt} - T_S^t)/\Delta t$; where T_S^t is the surface temperature at the previous time step), the snow melt heat flux Q_m is

$$Q_m = \max(Q_a(T_{melt}) - \frac{c_{top}\ z_{top}}{\Delta t}\ (T_{melt} - T_S^t),\ \frac{W_{snow}\ L_f}{\Delta t}) \tag{3.101}$$

where W_{snow} is the mass of the snow water of the total snow pack and L_f is the latent heat of fusion. Any excess of energy is used to warm the soil.

With the heat flux F_z at depth z of the soil

$$F_z = -k\ \frac{\partial T}{\partial z} \tag{3.102}$$

one dimensional energy conservation requires

$$c\ \frac{\partial T}{\partial t} = -\frac{\partial F_z}{\partial z} = \frac{\partial}{\partial z}\left[k\ \frac{\partial T}{\partial z}\right] \tag{3.103}$$

where c is the volumetric soil heat capacity, T is the soil temperature, and k is the thermal conductivity.

In the model, thermal properties (temperature, thermal conductivity, volumetric heat capacity) are defined at the center of each layer. Assuming the heat flux from i to the interface i and $i+1$ equals the heat flux from the interface to $i+1$, the heat flux F_i from layer i to layer $i+1$ (positive downwards) is given by

$$F_i = -\frac{2\ k_i\ k_{i+1}(T_i - T_{i+1})}{k_{i+1}\ \Delta z_i + k_i\ \Delta z_{i+1}} \tag{3.104}$$

The energy balance for layer i is

$$\frac{c_i\ \Delta z_i}{\Delta t}\ (T_i^{t+\Delta t} - T_i^t) = F_i - F_{i-1} \tag{3.105}$$

The boundary conditions are zero flux at the bottom of the soil column and heat flux F_g at the top.

This equation is solved implicitly using fluxes F_i evaluated at $t + \Delta t$

$$\begin{aligned}
\frac{c_i \Delta z_i}{\Delta t}(T_i^{t+\Delta t} - T_i^t) &= \frac{k_i k_{i+1}(T_{i+1}^{t+\Delta t} - T_i^{t+\Delta t})}{k_{i+1}\Delta z_i + k_i \Delta z_{i+1}} + G && for \quad i = 1 \\
\frac{c_i \Delta z_i}{\Delta t}(T_i^{t+\Delta t} - T_i^t) &= \frac{k_i k_{i+1}(T_{i+1}^{t+\Delta t} - T_i^{t+\Delta t})}{k_{i+1}\Delta z_i + k_i \Delta z_{i+1}} + \frac{k_i k_{i-1}(T_{i-1}^{t+\Delta t} - T_i^{t+\Delta t})}{k_{i-1}\Delta z_i + k_i \Delta z_{i-1}} && for \quad 1 < i < N \\
\frac{c_i \Delta z_i}{\Delta t}(T_i^{t+\Delta t} - T_i^t) &= \frac{k_i k_{i-1}(T_{i-1}^{t+\Delta t} - T_i^{t+\Delta t})}{k_{i-1}\Delta z_i + k_i \Delta z_{i-1}} && for \quad i = N
\end{aligned} \tag{3.106}$$

resulting in a linear system for the $T_i^{t+\Delta t}$.

3.5.2 Soil Hydrology

The parameterization of soil hydrology comprises the budgets for snow amount and the soil water amount. The water equivalent of the snow layer $z_{snow}^{H_2O}$ is computed over land and glacier areas from

$$\frac{\partial z_{snow}^{H_2O}}{\partial t} = F_q + P_{snow} - M_{snow} \tag{3.107}$$

where F_q is the evaporation rate over snow computed from Eq. 3.4, P_{snow} is the snow fall and M_{snow} is the snow melt rate (all fluxes are positive downward and in m/s). M_{snow} is related to the snow melt heat flux Q_m (Eq. 3.101) by

$$M_{snow} = \frac{Q_m}{\rho_{H_2O} L_f} \tag{3.108}$$

where L_f is the latent heat of fusion.

The soil water reservoir W_{soil} [m] is represented by a single-layer bucket model (Manabe 1969). Soil water is increased by precipitation P and snow melt M_{snow} and is depleted by the surface evaporation F_q:

$$\frac{\partial W_{soil}}{\partial t} = P + M + F_q \tag{3.109}$$

where all fluxes are defined positive downwards and in m/s. Soil water is limited by a field capacity W_{max} which geographical distribution can be prescribed via an external input or is set to a default value of 0.5 m everywhere. If the soil water exceeds W_{max} the excessive water builds the runoff R and is provided to the river transport scheme (Section 3.5.3). The ratio of the soil water and the field capacity defines the wetness factor C_w which is used in Eq. 3.4 to compute the surface evaporation:

$$C_w = \frac{W_{soil}}{f_{Cw} W_{max}} \tag{3.110}$$

where the factor f_{Cw} (with a default value of 0.25) takes into account that maximum evaporation will take place even if the bucket is not completely filled. For land points covered by glaciers, C_w is set to a constant value of 1.

3.5.3 River Transport

The local runoff is transported to the ocean by a river transport scheme with linear advection (Sausen et al. 1994). For each grid box (both, land and ocean costal points) the river water amount W_{river} [m^3] is computed from

$$\frac{\partial W_{river}}{\partial t} = ADV + area\ (R - S) \tag{3.111}$$

where R is the local runoff (Section 3.5.2), S is the input into the ocean, ADV is the advection of river water and $area$ is the area of the respective grid box. The input into the ocean S is given by

$$S = \begin{cases} 0 & \text{for land points} \\ \\ ADV & \text{for ocean points} \end{cases} \tag{3.112}$$

This ensures that S is non-zero only for ocean costal points. The advection from grid box (i,j) into grid box (i',j'), $ADV_{(i,j)\rightarrow(i',j')}$, is formulated using an upstream scheme:

$$\begin{aligned} ADV_{(i,j)\rightarrow(i+1,j)} &= \begin{cases} u_{i,j} W_{i,j}, & \text{if } u_{i,j} \geq 0 \\ \\ u_{i,j} W_{i+1,j}, & \text{if } u_{i,j} < 0 \end{cases} \\ \\ ADV_{(i,j)\rightarrow(i,j+1)} &= \begin{cases} -v_{i,j} W_{i,j}, & \text{if } v_{i,j} \leq 0 \\ \\ -v_{i,j} W_{i,j+1}, & \text{if } v_{i,j} > 0 \end{cases} \end{aligned} \tag{3.113}$$

where i and j are the zonal and meridional indices of the grid box, which are counted from the west to the east and from the north to the south, respectively. The zonal and meridional advection rates $u_{i,j}$ and $v_{i,j}$ are defined at the interface of two grid boxes and depend on the slope of the orography:

$$\begin{aligned} u_{i,j} &= \frac{c}{\Delta x}\left[\frac{h_{i,j}-h_{i+1,j}}{\Delta x}\right]^{\alpha} \\ v_{i,j} &= \frac{c}{\Delta y}\left[\frac{h_{i,j+1}-hi,j}{\Delta y}\right]^{\alpha} \end{aligned} \tag{3.114}$$

where Δx and Δy are the distances between the grid points in the longitudinal and the meridional direction. h is the height of the orography, which is modified in order to omit local minima at land grid points. The empirical constants c and α are set to the values given by Sausen et al. (1994) for T21 resolution ($c = 4.2$ m/s and $\alpha = 0.18$).

3.5.4 Other Land Surface Parameter

Some additional quantities characterizing the land surface of each grid box need to be specified for use in the model. The land-sea mask and the orography are read from an external file. Optionally, this file may also include other climatological surface parameter: the global distribution of the surface roughness length z_0, a background albedo $\mathcal{R}_S^{clim}$, a glacier mask for permanent ice sheets, the bucked size for the soil water W_{max} (see section above) and a climatological annual cycle of the soil wetness C_w^{clim} (which may be used instead of the computed C_w from Eq. 3.110. If there is no input for the particular field in the file, the parameter is set to be horizontal homogeneous with a specific value. The following defaults are used: $z_0 =$ 2 m, $\mathcal{R}_S^{clim} = 0.2$, no glaciers, $W_{max} = 0.5$ and $C_w^{clim} = 0.25$.

For snow covered areas, the background albedo is modified to give the actual albedo $\mathcal{R}_S$ which is used in the radiation scheme. For points, which are not covered by glaciers, $\mathcal{R}_S$ is given by

$$\mathcal{R}_S = \mathcal{R}_S^{clim} + (\mathcal{R}_S^{snow} - \mathcal{R}_S^{clim})\,\frac{z_{snow}}{z_{snow}+0.01} \tag{3.115}$$

where z_{snow} is the snow depth, and the albedo of the snow, $\mathcal{R}_S^{snow}$, depends on the surface temperature T_S

$$\mathcal{R}_S^{snow} = \mathcal{R}_{max}^{snow} + (\mathcal{R}_{min}^{snow} - \mathcal{R}_{max}^{snow})\,\frac{T_S - 263.16}{10} \tag{3.116}$$

with $\mathcal{R}_{min}^{snow} \le \mathcal{R}_S^{snow} \le \mathcal{R}_{max}^{snow}$ and default values $\mathcal{R}_{min}^{snow} = 0.4$ and $\mathcal{R}_{max}^{snow} = 0.8$.
For glaciers, $\mathcal{R}_S$ is given by $\mathcal{R}_S^{snow}$ from Eq. 3.116 but with a default $calR_{min}^{snow} = 0.6$.
The surface specific humidity q_S is given by the saturation specific humidity at T_S:

$$q_S = q_{sat}(T_S) \tag{3.117}$$

where $q_{sat}(T_S)$ is computed from Eq. 3.73.

3.6 Sea Surface

Sea surface temperatures T_{sea}, sea ice distributions c_{ice} and surface temperatures over sea ice T_i are provided by the ocean and sea ice modules (Section HEIKO). From these quantities, the following additional parameter are computed which enter the atmospheric parameterizations.

The prescribed surface albedo $\mathcal{R}_{\mathcal{S}}$ for open water is set to a default value of 0.069. For sea ice $\mathcal{R}_S$ is given as a function of the ice surface temperature T_i:

$$\mathcal{R}_S = \min\left(\mathcal{R}_S^{max},\, 0.5 + 0.025\,(273. - T_i)\right) \tag{3.118}$$

where the prescribed maximum sea ice background albedo $\mathcal{R}_S^{max}$ is set to a default value of 0.7.

The surface specific humidity q_S is given by the saturation specific humidity at the surface temperature T_S which is either T_{sea} or T_i:

$$q_S = q_{sat}(T_S) \tag{3.119}$$

where $q_{sat}(T_S)$ is computed from Eq. 3.73. The wetness factor C_w which enters the calculation of the surface evaporation (Eq. 3.4) is set to 1.

The roughness length z_0 over sea ice is set to a constant value of $z_0 = 0.001$ m. Over open water, z_0 is computed from the Charnock (1955) formula:

$$z_0 = C_{char}\frac{u_*^2}{g} \tag{3.120}$$

with a minimum value of $1.5 \cdot 10^{-5}$ m. C_{char} denotes the Charnock constant and is set to 0.018. g is the gravitational acceleration. The friction velocity u_* is calculated from the surface wind stress at the previous time level:

$$u_* = \sqrt{\frac{|F_u, F_v|}{\rho}} \tag{3.121}$$

where $|F_u, F_v|$ is the absolute value of the surface wind stress computed from Eq. 3.4 and ρ is the density.

3.7 References

Berger, A., 1978a: A simple algorithm to compute long-term variations of daily insolation. Institute of Astronomy and Geophysic, Universite Catholique de Louvain, **Contribution 18**, Louvain-la-Neuve, Belgium.

Berger, A., 1978b: Long-term variations of daily insolation and quaternary climatic change. *J. Atmos. Sci.*, **35**, 2362- 2367.

Blackadar, A. K., 1962: The vertical distributionof wind and turbulent exchange in a neutral atmosphere. *J. Geophys. Res.*, **67**, 3095-3102.

Boer, G. J., N. A. McFarlane, R. Laprise, J. Henderson and J.-P. Blanchet, 1984: The Canadian Climate Centre spectral atmospheric general circulation model. *Atmosphere-Ocean*, **22**, 397-429.

Charnock, M., 1955: Wind stress on a water surface. *Q. J. R. Meteorol. Soc.*, **81**, 639-640.

Chou, M.-D., M. J. Suarez, X.-Z. Liang and M. M. H. Yan, 2001 (Revised 2002): A thermal infrared radiation parameterization for atmospheric studies. *Technical Report Series on Global Modelling and Data Assimilation, M. J. Suarez Ed.*, **NASA/TM-2001-104606, Vol. 19**, 55pp.

Green, A. E. S., 1964: Attenuation by ozone and the earth's albedo in the middle ultraviolet. *AAppl. Opt.*, **3**, 203-208.

Katayama, A., 1972: A simplified scheme for computing radiative transfer in the troposphere. Department of Meteorology, *Tech. Report*, **No. 6**, University of California, Los Angeles, CA, 77 pp.

Kiehl, J. T., J. J. Hack, G. B. Bonan, B. A. Boville, B. P. Briegleb, D. L. Williamson and P. J. Rasch, 1996: Description of the NCAR Community Climate Model (CCM3). *NCAR Technical Note*, **NCAR/TN-420+STR**, 152pp.

Kuo, H. L., 1965: On formation and intensification of tropical cyclones through latent heat release by cumulus convection. *J. Atmos. Sci.*, **22**, 40-63.

Kuo, H. L., 1974: Further studies of the parameterization of the influence of cumulus convection on large-scale flow. *J. Atmos. Sci.*, **31**, 1232-1240.

Lacis, A. A., and J. E. Hansen, 1974: A parameterization for the absorption of solar radiation in the Earth's atmosphere. *J. Atmos. Sci.*, **31**, 118-133.

Laurson, L. and E. Eliasen, 1989: On the effects of the damping mechanisms in an atmospheric general circulation model. *Tellus*, **41A**, 385-400.

Louis, J. F., 1979: A parametric model of vertical eddy fluxes in the atmosphere. *Boundary Layer Meteorology*, **17**, 187-202.

Louis, J. F., M. Tiedtke and M. Geleyn, 1982: A short history of the PBL parameterisation at ECMWF. Proceedings, ECMWF workshop on planetary boundary layer parameterization, Reading, 25-27 Nov. 81, 59-80.

Lowe, P. R., 1977: An approximating polynomial for the computation of saturation vapour pressure. *J. Appl. Met.*, **16**, 100-103.

Manabe, S. and F. Möller, 1961: on the radiative equilibrium and heat balance of the atmosphere. *Mon Wea. Rev.*, **89**, 503-532.

Manabe, S., 1969: Climate and ocean circulation. I. The atmospheric circulation and the hydrology of the earth's surface. *Mon. Wea. Rev.*, **97**, 739-774.

Rodgers, C. D., 1967: The use of emissivity in the atmospheric radiation calculation. *Q. J. R. Meteorol. Soc.*, **93**, 43-54.

Roeckner, E., K. Arpe, L. Bengtsson, S. Brinkop, L. Dümenil, M. Esch, E. Kirk, F. Lunkeit, M. Ponater, B. Rockel, R. Sausen, U. Schlese, S. Schubert and M. Windelband, 1992: Simulation of the present-day climate with the ECHAM-3 model: Impact of model physics and resolution. Max-Planck Institut für Meteorologie, **Report No. 93**, 171pp.

Sasamori, T., 1968: The radiative cooling calculation for application to general circulation experiments. *J. Appl. Met.*, **7**, 721-729.

Sausen, R., S. Schubert and L. Dümenil, 1994: A model of river runoff for use in coupled atmosphere-ocean models. *Journal of Hydrology*, **155**, 337-352.

Slingo, A., and J. M. Slingo, 1991: Response of the National Center for Atmospheric Research community climate model to improvements in the representation of clouds. *J. Geoph. Res.*, **96**, 341-357.

Stephens, G. L., 1978: Radiation profiles in extended water clouds. II: Parameterization schemes. *J. Atmos. Sci.*, **35**, 2123-2132.

Stephens, G. L., 1984: The parameterization of radiation for numerical weather prediction and climate models. *Mon. Wea. Rev.*, **112**, 826-867.

Stephens, G. L., S. Ackermann and E. A. Smith, 1984: A shortwave parameterization revised to improve cloud absorption. *J. Atmos. Sci.*, **41**, 687-690.

Chapter 4

Equations

4.1 Pressure coordinate

The primitive equations in the (λ, μ, p) -coordinates without scaling. That means D and *zeta* in Appendix A and B have the units: $s^{-}1$, T is in K, p in Pa, ϕ in $m^2 s^{-2}$ and $\vec{\nu}$ in ms^{-1}.

Conservation of momentum (vorticity and divergence equation)

$$\frac{\partial \zeta}{\partial t} = -\vec{\nu} \cdot \bigtriangledown(\zeta + f) - \omega \frac{\partial \zeta}{\partial p} - (\zeta + f) \bigtriangledown \cdot \vec{\nu} + \vec{k} \cdot (\frac{\partial \vec{\nu}}{\partial p} \times \bigtriangledown \omega) + P_\zeta \tag{4.1}$$

$$\frac{\partial D}{\partial t} = \vec{k} \cdot \bigtriangledown \times (\zeta + f)\vec{\nu} - \bigtriangledown \cdot (\omega \frac{\partial \vec{\nu}}{\partial p}) - \bigtriangledown^2(\phi + \frac{\vec{\nu}^2}{2}) + P_D \tag{4.2}$$

Hydrostatic approximation (using the equation of state)

$$\frac{\partial \phi}{\partial p} = -\frac{1}{\rho} = -\frac{RT}{p} \tag{4.3}$$

Conservation of mass (continuity equation)

$$\bigtriangledown \cdot \vec{\nu} + \frac{\partial \omega}{\partial p} = 0 \tag{4.4}$$

Thermodynamic equation (J= diabatic heating per unit mass)

$$\frac{dT}{dt} = \frac{\omega}{c_p \rho} + \frac{J}{c_p} + P_T \tag{4.5}$$

4.2 Sigma-system

$\sigma = p/p_s$ ranges monotonically from zero at the top of the atmosphere to unity at the ground. For $\xi = x, y$ or t

$$(\frac{\partial}{\partial \xi})_p = \frac{\partial}{\partial \xi} - \sigma \frac{\partial \ln p_s}{\partial \xi} \frac{\partial}{\partial \sigma} \tag{4.6}$$

$$\frac{\partial}{\partial p} = \frac{\partial \sigma}{\partial p} \frac{\partial}{\partial \sigma} = \frac{1}{p_s} \frac{\partial}{\partial \sigma} \tag{4.7}$$

The vertical velocity in the p-coordinate system ω and in the new σ-coordinate system $\dot{\sigma}$ are given by [Phillips (1957)]

$$\omega = \frac{p}{p_s}[\vec{V}\cdot\nabla p_s - \int_0^\sigma \nabla\cdot p_s\vec{V}d\sigma] = p[\vec{V}\cdot\nabla\ln p_s] - p_s\int_0^\sigma Ad\sigma \tag{4.8}$$

$$\dot{\sigma} = \sigma\int_0^1 Ad\sigma - \int_0^\sigma Ad\sigma \tag{4.9}$$

with $A = D + \vec{V}\cdot\nabla\ln p_s = \frac{1}{p_s}\nabla\cdot p_s\vec{V}$.
The primitive equations in the (λ,μ,σ) -coordinates without scaling
Conservation of momentum (vorticity and divergence equation)

$$\frac{\partial\zeta}{\partial t} = \frac{1}{a(1-\mu^2)}\frac{\partial F_\nu}{\partial\lambda} - \frac{1}{a}\frac{\partial F_u}{\partial\mu} + P_\zeta \tag{4.10}$$

$$\frac{\partial D}{\partial t} = \frac{1}{a(1-\mu^2)}\frac{\partial F_u}{\partial\lambda} + \frac{1}{a}\frac{\partial F_\nu}{\partial\mu} - \bigtriangledown^2(E+\phi+T_0\ln p_s) + P_D \tag{4.11}$$

Hydrostatic approximation (using the equation of state)

$$\frac{\partial\phi}{\partial\ln\sigma} = -TR \tag{4.12}$$

Conservation of mass (continuity equation)

$$\frac{\partial\ln p_s}{\partial t} = -\frac{U}{a(1-\mu^2)}\frac{\partial\ln p_s}{\partial\lambda} - \frac{V}{a}\frac{\partial\ln p_s}{\partial\mu} - D - \frac{\partial\dot{\sigma}}{\partial\sigma} = -\int_0^1(D+\vec{V}\cdot\nabla\ln p_s)d\sigma \tag{4.13}$$

Thermodynamic equation (J= diabatic heating per unit mass)

$$\frac{\partial T}{\partial t} = F_T - \dot{\sigma}\frac{\partial T}{\partial\sigma} + \kappa T[\vec{V}\cdot\nabla\ln p_s - \frac{1}{\sigma}\int_0^\sigma Ad\sigma] + \frac{J}{c_p} + P_T \tag{4.14}$$

$E = \dfrac{U^2+V^2}{2(1-\mu^2)}$
$F_u = (\zeta+f)V - \dot{\sigma}\dfrac{\partial U}{\partial\sigma} - \dfrac{RT}{a}\dfrac{\partial\ln p_s}{\partial\lambda}$
$F_\nu = -(\zeta+f)U - \dot{\sigma}\dfrac{\partial V}{\partial\sigma} - (1-\mu^2)\dfrac{RT}{a}\dfrac{\partial\ln p_s}{\partial\mu}$
$F_T = -\dfrac{U}{a(1-\mu^2)}\dfrac{\partial T}{\partial\lambda} - \dfrac{V}{a}\dfrac{\partial T}{\partial\mu}$
$A = D + \vec{V}\cdot\nabla\ln p_s = \frac{1}{p_s}\nabla\cdot p_s\vec{V}$.

4.3 Matrix $\boldsymbol{B}$

For the implicit scheme, fast (linear) gravity modes and the slower non-linear terms are separated.

$$\frac{\partial D}{\partial t} = N_D - \bigtriangledown^2(\phi + T_0\ln p_s)$$

$$\frac{\partial\ln p_s}{\partial t} = N_p - \int_0^1 Dd\sigma$$

$$\frac{\partial T'}{\partial t} = N_T - [\sigma \int_0^1 D d\sigma - \int_0^\sigma D d\sigma] \frac{\partial T_0}{\partial \sigma} + \kappa T_0 [- \int_0^\sigma D d \ln \sigma]$$

$$\frac{\partial \phi}{\partial \ln \sigma} = -T$$

The set of differential equations are approximated by its finite difference analogues using the notation (for each variable D, T, $\ln p_s$, and ϕ)

$$\overline{Q}^t = 0.5(Q^{t+\Delta t} + Q^{t-\Delta t}) = Q^{t-\Delta t} + \Delta t \delta_t Q$$

and

$$\delta_t Q = \frac{Q^{t+\Delta t} - Q^{t-\Delta t}}{2\Delta t}$$

The hydrostatic approximation using an angular momentum conserving finite-difference scheme is solved at half levels

$$\phi_{r+0.5} - \phi_{r-0.5} = T_r \cdot \ln \frac{\sigma_{r+0.5}}{\sigma_{r-0.5}}$$

Full level values of geopotential are given by

$$\phi_r = \phi_{r+0.5} + \alpha_r T_r \text{ with } \alpha_r = 1 - \frac{\sigma_{r-0.5}}{\Delta \sigma_r} \ln \frac{\sigma_{r+0.5}}{\sigma_{r-0.5}} \text{ and } \Delta \sigma_r = \sigma_{r+0.5} - \sigma_{r-0.5}$$

Now, the implicit formulation for the divergence is derived using the conservation of mass, the hydrostatic approximation and the thermodynamic equation at discrete time steps

$$\delta_t D = N_D - \nabla^2 (\overline{\phi}^t + T_0 [\ln p_s^{t-\Delta t} + \Delta t \delta_t \ln p_s])$$

$$\delta_t \ln p_s = N_p - L_p [D^{t-\Delta t} + \Delta t \delta_t D]$$

$$\overline{\phi - \phi_s}^t = L_\phi [T^{t-\Delta t} + \Delta t \delta_t T]$$

$$\delta_t T' = N_T - L_T [D^{t-\Delta t} + \Delta t \delta_t D]$$

The set of differential equations for each level $k (k = 1, .., n)$ written in vector form leads to the matrix $\mathcal{B}$ with n rows and n columns. The matrix $\mathcal{B} = \mathcal{L}_\phi \mathcal{L}_T + \vec{T}_0 \vec{L}_p = \mathcal{B}(\sigma, \kappa, \vec{T}_0)$ is constant in time. The variables $\vec{D}, \vec{T}, \vec{T}', \vec{\phi} - \vec{\phi}_s$ $\vec{N}_D$ and $\vec{N}_T$ are represented by column vectors with values at each level. L_p, L_T and L_ϕ contain the effect of the divergence (or the gravity waves) on the surface pressure tendency, the temperature tendency and the geopotential.

$\vec{L}_p = (\Delta \sigma_1, ..., \Delta \sigma_n)$ is a row vector with $\Delta \sigma_n = \sigma_{n+0.5} - \sigma_{n-0.5}$.

$$\mathcal{L}_\phi = \begin{pmatrix} 1 & \alpha_{21} & \alpha_{31} & \cdots & \alpha_{n1} \\ 0 & \alpha_{22} & \alpha_{32} & \ddots & \vdots \\ \vdots & \vdots & \vdots & \ddots & \vdots \\ 0 & 0 & \cdots & 0 & \alpha_{nn} \end{pmatrix}$$

For $i = j : \alpha_{jj} = 1 - [\frac{\sigma_{j-0.5}}{\sigma_{j+0.5} - \sigma_{j-0.5}} (\ln \sigma_{j+0.5} - \ln \sigma_{j-0.5})]$

$i > j : \alpha_{ij} = \ln \sigma_{j+0.5} - \ln \sigma_{j-0.5}$

$i < j : \alpha_{ij} = 0.$

$$\mathcal{L}_T = \begin{pmatrix} \kappa(T_0)_1\alpha_{11} & \kappa(T_0)_1\alpha_{21} & \cdots & \kappa(T_0)_1\alpha_{n1} \\ \kappa(T_0)_2\alpha_{12} & \kappa(T_0)_2\alpha_{22} & \ddots & \vdots \\ \vdots & \vdots & \ddots & \vdots \\ \kappa(T_0)_n\alpha_{1n} & \kappa(T_0)_n\alpha_{2n} & \cdots & \kappa(T_0)_n\alpha_{nn} \end{pmatrix} + \begin{pmatrix} \gamma_{11} & \gamma_{21} & \gamma_{31} & \cdots & \gamma_{n1} \\ \gamma_{12} & \gamma_{22} & \gamma_{32} & \ddots & \vdots \\ \vdots & \vdots & \vdots & \ddots & \vdots \\ \gamma_{1n} & \gamma_{2n} & \cdots & \cdots & \gamma_{nn} \end{pmatrix}$$

$\tau_{ij} = \kappa(T_0)_j\alpha_{ij} + \gamma_{ij}$ with $\Delta T_{n+0.5} = (T_0)_{n+1} - (T_0)_n$

for $j = 1$ and
$i = j$: $\gamma_{jj} = \frac{1}{2}[\Delta T_{0.5}(\sigma_1 - 1)]$

$i > j$: $\gamma_{ij} = \frac{1}{2}\Delta\sigma_i[\Delta T_{0.5}\sigma_1]$

for $j > 1$ and
$i = j$: $\gamma_{jj} = \frac{1}{2}[\Delta T_{j-0.5}\sigma_{j-0.5} + \Delta T_{j+0.5}(\sigma_{j+0.5} - 1)]$

$i < j$: $\gamma_{ij} = \frac{\Delta\sigma_i}{2\Delta\sigma_j}[\Delta T_{j-0.5}(\sigma_{j-0.5} - 1) + \Delta T_{j+0.5}(\sigma_{j+0.5} - 1)]$

$i > j$: $\gamma_{ij} = \frac{\Delta\sigma_i}{2\Delta\sigma_j}[\Delta T_{j-0.5}\sigma_{j-0.5} + \Delta T_{j+0.5}\sigma_{j+0.5}]$

Part II

Ocean: Mixed Layer

Chapter 5

Slab Ocean Model

The slab ocean model consists of a prognostic equation at each ocean point for the oceanic mixed-layer temperature T_{mix}. The communication between the gridpoints is approximated by the climatological heat flux Q_c. For the Kraus-Turner type model also the mixed layer depth h_{mix} is calculated using the tubulent kinetic energy (TKE) and the buoyancy budget.

5.1 Constant-depth mixed layer and flux correction

The oceanic mixed layer integrates over the atmospheric heat fluxes Q_{atmos} which is the net atmosphere to ocean heat flux, which in the absence of the ice is defined as the sum of solar flux absorbed by the ocean, long wave cooling flux, sensible heat flux from the ocean into the atmosphere, and latent heat flux from ocean to atmosphere.

$$\frac{dT_{mix}}{dt} = \frac{Q_{atmos} + Q_c}{\rho_w c_{p_w} h_{mix}} \tag{5.1}$$

The mixed layer depth h_{mix} is fixed to 50 m or prescribed by a climatological seasonal cycle. The impact of oceanic heat transport Q_c on the sea surface temperature (SST) can be approximated in to ways. First, it can be calculated by the difference of the longterm average (denoted by <>) of the atmospheric heat fluxes Q_{atmos} and the climatological temperature change (Q_{c_1}).

$$Q_{c_1} =< Q_{atmos} > - < \frac{dT_{mix}}{dt} \rho_w c_{p_w} h_{mix} > \tag{5.2}$$

Second, this parameterization is similar to the traditional flux correction Q_{c_2}.

$$Q_{c_2} = \rho_w c_{p_w} h_{mix} \frac{T_{mix_c} - T_{mix}}{\tau_T} \tag{5.3}$$

Here, the time scales τ_T is about 50 days.

5.2 Kraus-Turner type model

The integral mixed layer ocean model predicts the evolution of the integrated properties of the upper ocean layer [Kraus (1967), Gaspar (1988)]. The Kraus-Turner type model is modified including the contribution of thermocline processes to the buoyancy budget of the upper ocean [Karaca and Müller (1991), Dommenget and Latif (2000)]. The temperature distribution $T_{oz}(z)$, z is the depth, is approximated by

$$T_w(z) = T_{ref} + (T_{mix} - T_{ref}) e^D \tag{5.4}$$

T_{ref} is the asymptotic reference temperature and T_d the temperature at the bottom of the column in the depth ($z = -h$).

$D = \frac{z + h_{mix}}{h - h_{mix}} \ln(\frac{T_{mix} - T_{ref}}{T_d - T_{ref}})$ and $e^D = (\frac{T_{mix} - T_{ref}}{T_d - T_{ref}})^{(z+h_{mix})/(h-h_{mix})}$

Changes of buoyancy and potential energy in the total column can be measured by the zeroth and first moment of the temperature distribution (N=0,1)

$$R_N = \int_{-h}^{0} dz(T_w - T_{ref})(-z)^N \tag{5.5}$$

The buoyancy budget is changed by surface heat fluxes

$F_q = \frac{dR_0}{dt} = \frac{Q_{atmos}}{c_{p_w}\rho_w}[\frac{Km}{s}]$

$F_q^* = \rho_w c_{p_w} F_q = Q_{atmos}[\frac{W}{m^2} = \frac{kg}{s^2}]$

The turbulent kinetic energy (TKE) F_p provides the work necessary to change the potential energy of the total column

$F_p = \frac{dR_1}{dt} = \frac{m\rho}{g\alpha\rho_w} u_*^3 (\frac{\rho}{\rho_w})^{\frac{1}{2}} + 0.5 H_p F_q [\frac{Km^2}{s}]$

$F_p^* = \alpha g \rho_w F_p = m\rho u_*^3 (\frac{\rho}{\rho_w})^{\frac{1}{2}} + \frac{\alpha g}{c_{p_w}} 0.5 H_p F_q^* [\frac{W}{m^2 s} = \frac{kg}{s^3}]$

The wind generated TKE can be parameterized in terms of the atmospheric friction velocity u_* describing the work necessary to dislocate the center of gravity, keeping the total buoyancy fixed. This dislocation is essentially a consequence of the entrainment processes at the mixed layer base. The other term on the right side of the TKE budget denotes the work necessary to distribute the buoyancy, supplied at the surface, over the whole system for fixed center of gravity. For $m = 16$ the redistribution by transport and pressure forces and the mechanical production has a realistic impact on the TKE budget [Kraus (1967), Gaspar (1988)]. Here, salinity effects are ignored; assuming the familiar linear relationship between density ρ_w and temperature for sea water $\rho_w = \rho_{w_0}[1 - \alpha(T - T_{ref})]$ with the thermal expansion coefficient α, a constant density ρ_{w_0} and the reference temperature T_{ref}. The effective mixed layer depth H_q and the reduced center of gravity H_p is given by $H_q = \frac{R_0}{T_{mix} - T_{ref}}[m]$ and $H_p = \frac{R_1}{R_0}[m]$.

Using these definitions the prognostic equations for the mixed layer temperature and depth are

$$\frac{dT_{mix}}{dt} = \frac{F_q(h_{mix} + 0.5H_p) - F_p}{H_q h_{mix}} + \frac{Q_c}{\rho_w c_{p_w} h_{mix}} \tag{5.6}$$

$$\frac{dh_{mix}}{dt} = \frac{(F_p - 0.5 H_p F_q)}{(T_{mix} - T_{ref} - \Theta_2) h_{mix}} + \frac{h_{mix_c} - h_{mix}}{\tau_h} \tag{5.7}$$

with $\Theta_2 = (T_{mix} - T_d) / \ln(\frac{(T_{mix} - T_{ref})}{(T_d - T_{ref})})$

The time scales τ_h are about 50 days. The climatological heat flux Q_c is defined in the section before For detrainment ($w_e = 0$) the temperature derived from a surface heat flux relationship using a constant or climatological mixed layer depth (see previous section).

Appendix

Parameter	Symbol	Value
acceleration of gravity	g	$9.81\,\mathrm{m\,s^{-2}}$
density of sea water	ρ_w	$1030\,\mathrm{kg\,m^{-3}}$
specific heat of sea water	c_{p_w}	$4180\,\mathrm{W\,s\,kg^{-1}\,K^{-1}}$
thermal expansion coefficient	$\alpha = \frac{1}{\rho}\frac{d\rho}{dT}$	$2.41 \cdot 10^{-4}\ \mathrm{K^{-1}}$

Table 5.1: Thermodynamic parameters for the mixed layer model.

Part III

Biosphere: SIMBA

Chapter 6

Dynamic Vegetation

A simple dynamic parameterization is used to calculate the dynamics of those land surface parameters which are strongly affected by terrestrial vegetation. These parameters include the background albedo of the surface A, the roughness length z_0, the stress factor for the latent heat flux C_w, and the depth of the rooting zone W_{max}. These parameters are simulated as functions of two carbon pools, a fast pool to represent leaf area which responds quickly to changes in environmental conditions, and a slow pool to represent woody biomass which responds to changes in environmental conditions on a climatic time scale.

6.1 Vegetative Cover

The vegetative cover f_{veg} of the land surface, that is the fraction which is covered by green biomass (leaves), is computed as the minimum of an environmentally limited value $f_{veg,e}$ and a structurally limited value $f_{veg,e}$:

$$f_{veg} = \min\left(f_{veg,e}, f_{veg,s}\right) \tag{6.1}$$

The environmentally limited vegetation cover $f_{veg,e}$ is computed from the surface temperature T_S and from soil moisture W_{soil} as:

$$f_{veg,e} = f_{W_{soil}}\, f_{T_S} \tag{6.2}$$

with the two functions $f_{W_{soil}}$ and f_{T_S} given by:

$$f_W = \min\left(1, \max\left(0, \frac{W_{soil}/W_{max}}{W_{crit}}\right)\right) \tag{6.3}$$

$$f_T = \min\left(1, \max\left(0, \frac{T_S - T_{melt}}{T_{crit}}\right)\right) \tag{6.4}$$

with values of W_{crit}=0.25 and T_{crit}=293 K. The water limitation function f_W is motivated by the fact that water stress for plants sets in at a critical value W_{crit}. For simplicity, a fractional water content is used rather than a specific matric potential which would reflect the permanent wilting point.

The structurally limited vegetation cover $f_{veg,s}$ is obtained from a maximum leaf area index LAI_{max}

$$f_{veg,s} = 1 - \exp\left(-k\, LAI_{max}\right) \tag{6.5}$$

which is sustained with the present amount of biomass, as expressed by the amount of forest cover f_{forest}:

$$LAI_{max} = f_{forest}\, LAI_{forest} + (1 - f_{forest})\, LAI_{grass} \tag{6.6}$$

with values for maximum leaf area indices of LAI_{grass}=2 and LAI_{forest}=6. With this formulation, a land surface with no forest cover can only obtain a maximum value of LAI_{grass}, which is set to a typical maximum value for grassland. With full forest cover, the maximum sustainable leaf area index is given by a typical maximum value for forests, LAI_{forest}.

6.2 Carbon Balance

The gross carbon uptake (gross primary production, GPP) is calculated from incoming solar radiation, vegetation cover and light use efficiency:

$$GPP = c_{lue} f_W f_T f_{veg} F{\downarrow_s} \tag{6.7}$$

with a value of $c_{lue} = 1.5\,10^{-9}$ kgC/J. Total respiration is calculated from a Q_{10} relationship and total biomass BM:

$$RES = c_{res} Q_{10}^{\frac{T_s - 283K}{10K}} BM \tag{6.8}$$

with a value of $c_res = 2.9\,10^{-9}$ kgC/m^2/s. The change in biomass BM is then computed as:

$$\frac{\partial BM}{\partial t} = GPP - RES \tag{6.9}$$

6.3 Derivation of Land Surface Parameters

Land surface parameters are derived directly from the vegetative cover and forest cover. Forest cover is calculated from total biomass as a non-linear relationship as:

$$f_{FOR} = \frac{atan(BM - c_a)/!c_b}{c_c} + c_d \tag{6.10}$$

with values of c_a=20 kgC, c_b=5 kgC, c_c=$\frac{\pi}{2} + atan(\frac{c_a}{c_b})$, and c_d=0.5. The other land surface parameters are calculated as:

$$\begin{aligned}
&LAI = -\tfrac{\ln(1-f_{veg})}{k} \\
&z_0 = f_{forest}\, z_{0,forest} + (1 - f_{forest})\, z_{0,bare} \\
&W_{max} = f_{forest}\, W_{max,forest} + (1 - f_{forest})\, W_{max,bare} \\
&A = f_{forest}\, A_{forest} + (1 - f_{forest})\, A_{bare} \\
&LAI_{max} = f_{forest} LAI_{forest} + (1 - f_{forest}) LAI_{grass} \\
&C_w = \begin{cases} \frac{GPP}{GPP_{max}} & \text{if } GPP_{max} > 0 \\ 0 & \text{otherwise} \end{cases}
\end{aligned} \tag{6.11}$$

with values of k=0.5, $z_{0,bare}$=0.05 m, $z_{0,forest}$=2 m, $W_{max,bare}$=0.05 m, $W_{max,forest}$=0.5 m, A_{bare}=0.35, and A_{forest}=0.12.

6.4 Model Calibration

The model is tuned to produce reasonable values of total vegetation biomass representative of tropical and temperate forests and to reproduce the relationship between forest cover and water availablility reasonably well. Key tuning parameters and their effects are:

Q_{10} A higher value reduces the latitudinal biomass gradient.

T_{crit} A higher value reduces biomass accumulation in higher latitudes.

c_a A higher value reduces the amount of forest cover. The value of c_a represents the amount of biomass required for a forest cover of 0.5.

c_b A higher value broadens the transition from forest to non-forested regions.

c_{res} A higher value reduces overall biomass.

Part IV

Ice

Chapter 7

Model Description

The sea ice model is based on the zero layer model of [Semtner (1976)]. This model computes the thickness of the sea ice from the thermodynamic balances at the top and the bottom of the sea ice. The zero layer assumes the temperature gradient in the ice to be linear and eliminates the capacity of the ice to store heat. Nevertheless, it has been used successfully in areas where ice is mostly seasonal and thus relatively thin ($< 1\,\mathrm{m}$) [Beckmann and Birnbaum (2001)]. Thus, the model is expected to perform better in the Southern Ocean than in the Arctic, where multiyear, thick ice dominates (cf. section 'Validation'). Sea ice is formed if the ocean temperature drops below the freezing point (271.25 K, cf. Eq. (7.1)) and is melted whenever the ocean temperature increases above this point. The prognostic variables are the sea ice temperature $T_i\,(\mathrm{K})$, the ice thickness $h_i\,(\mathrm{m})$ and the ice concentration A, which in the present model is boolean: A given grid point is either ice free ($A = 0$) or ice covered ($A = 1$). The freezing temperature $T_f\,(\mathrm{K})$ depends on salinity as [UNESCO (1978)]

$$T_f \;=\; 273.15 \;- 0.0575 S_w \;+ 1.7105 \times 10^{-3} S_w^{3/2} \;- 2.155 \times 10^{-4} S_w^2, \tag{7.1}$$

where $S_w\,(\mathrm{psu})$ denotes the salinity of sea water. On the range $0 < S_w < 40$, the salinity - freezing point dependency reduces to a linear relationship where T_f decreases with increasing salinity.

Freezing and melting of sea ice releases just the right amount of latent heat of fusion to close the energy balance with respect to the total heat flux $Q\,(\mathrm{W\,m^{-2}})$ in the mixed layer [Parkinson and Washington (1979)]:

$$Q \;+ \rho_i\, L_i\, \frac{dh_i}{dt} \;=\; 0, \tag{7.2}$$

where $\rho_i\,(\mathrm{kg\,m^{-3}})$ is the density of sea ice and $L_i\,(\mathrm{W\,m^{-1}\,K^{-1}})$ denotes the latent heat of fusion of sea ice. Standard parameter values are given in Table 7.1. [Parkinson and Washington (1979)] Thus, the prognostic equation for the sea ice thickness is given as

$$\frac{dh_i}{dt} = \frac{-Q}{\rho_i\, L_i}. \tag{7.3}$$

It is assumed that melting of sea ice takes place from above only, while freezing takes place at the lower side of the ice floe.

Basic equations

In the presence of sea ice, the heat fluxes are defined as follows. The total heat flux $Q\,(\mathrm{W\,m^{-2}})$ is given as

$$Q \;=\; Q_a \;+ Q_c \;+ Q_o \;+ \tilde{Q}, \tag{7.4}$$

where Q_a is the atmospheric heat flux, Q_c is the conductive heat flux through the ice, Q_o denotes the oceanic heat flux and $\tilde{Q}$ is the flux correction. The atmospheric heat flux

$$Q_a = \begin{cases} F_T + L + R_{s,\downarrow} + R_{s,\uparrow} + R_{l,\downarrow} + R_{l,\uparrow} & \text{if} \quad T_s > T_f, \\ 0 & \text{if} \quad T_s \leq T_f. \end{cases} \tag{7.5}$$

is the sum of sensible (F_T) and latent heat flux (L), the incoming and reflected short wave radiation ($R_{s,\downarrow}\, R_{s,\uparrow}$) and the long wave radiation (R_l). It is set to zero in the case of freezing, where the conductive heat flux applies (see below). The conductive heat flux through the ice

$$Q_c = \begin{cases} 0 & \text{if} \quad T_s > T_f, \\ \dfrac{\bar{\kappa}}{h_i + h_s}\,(T_s - T_f) & \text{if} \quad T_s \leq T_f. \end{cases} \tag{7.6}$$

is set to zero in the case of melting ice, as the ice melts at the top. If the ice is freezing, the atmospheric heat flux determines the surface temperature T_s and has to pass through the ice. Whatever energy is left at the bottom of the ice sheet is then available for freezing. $\bar{\kappa}\,(\mathrm{W\,m^{-1}\,K^{-1}})$ is the mean conductivity of the sea ice floe and snow cover, computed as

$$\bar{\kappa} = \frac{\kappa_i h_i + \kappa_s h_s}{h_i + h_s}. \tag{7.7}$$

The oceanic heat flux is considered only in the presence of sea ice:

$$Q_o = c_o\,(T_d - T_f). \tag{7.8}$$

It is determined by the gradient between the temperature of sea water in the deep ocean (T_d, (K)) and the surface temperature, which is the freezing temperature (T_f, (K)). In the absence of sea ice, the oceanic heat flux is implicitly considered as it determines the sea water temperature in the mixed layer (T_s, (K)). The flux correction is calculated as

$$\tilde{Q} = \frac{\rho_i\, L_i}{\varepsilon_c}\,(h_i - h_{i,c}), \tag{7.9}$$

where $h_{i,c}\,(\mathrm{m})$ is the climatological ice thickness and ε_c is a relaxation constant. For example, $\varepsilon = 2000$ corrects the ice thickness to climatological values in 2000 time steps.

In the case of melting ice, the ice thickness may become negative if the energy available for melting is greater than needed to melt the present ice. Then, the surplus energy is heating the sea water, setting the surface temperature to

$$T_s = T_f - \frac{\rho_i\, L_i\, h_i}{\rho_w\, c_{p_s}\, h_{mix}}, \tag{7.10}$$

with $h_i < 0$.

Ice formation from open water

If the surface temperature of open ocean water is below the freezing point, sea ice is formed. The heat flux available for freezing is given as

$$Q_f = \frac{\rho_w\, c_{p_w}\, h_{ml}}{dt}\,(T_s - T_f) + Q_{next}, \tag{7.11}$$

where $\rho_w\,(\mathrm{kg\,m^{-3}})$ is the density of sea water, $c_{p_w}\,(\mathrm{W\,s\,kg^{-1}\,K^{-1}})$ is the specific heat of sea water and $h_{ml}\,(\mathrm{m})$ denotes the mixed layer depth. The thickness of the new formed ice sheet

is calculated by setting $Q = Q_f + \tilde{Q}$ in (7.2). We have prescribed a minimum ice thickness $h_{i,min} = 0.1\,\mathrm{m}$, since the presence of sea ice drastically changes the albedo. Open ocean has an albedo of 0.1, whereas sea ice yields an albedo of 0.7. As the model differentiates only between no ice and full ice in one gridpoint, the albedo would change unrealistically early in the case of ice formation without the prescribed minimum thickness. If less than 10 cm ice is formed in one time step, the flux to form this amount of ice is taken to the next time step.Thus,

$$Q_{next} = \begin{cases} 0 & \text{if} \quad h_i \geq 0.1, \\ Q_f & \text{if} \quad h_i < 0.1. \end{cases} \tag{7.12}$$

If, for example, 4 cm ice is formed per time step and conditions do not change, it takes three time steps until the grid point is classified as ice covered.

Sea ice temperature

The sea ice temperature $T_i\,(\mathrm{K})$ is calculated from the energy balance at the ice surface:

$$(\rho_i\, c_{p_i}\, h_{min} + \rho_s\, c_{p_s}\, h_s)\frac{dT_i}{dt} - Q_b = 0 \;\Rightarrow\; \frac{dT_i}{dt} = \frac{Q_b}{\rho_i\, c_{p_i}\, h_{min} + \rho_s\, c_{p_s}\, h_s}, \tag{7.13}$$

where $Q_b = Q_a + Q_c$ with Q_a as defined in (7.5) and

$$Q_c = \frac{\bar{\kappa}}{h_i + h_s}\,(T_f - T_s) \tag{7.14}$$

$c_{p_i}, c_{p_s}\,(\mathrm{J\,kg^{-1}\,K^{-1}})$ are the specific heat of sea ice and snow, respectively. $h_s\,(\mathrm{m})$ denotes the snow depth. As far as the ice is concerned, only the upper 10 cm ($h_{min}\,(\mathrm{m})$) are taken into account here, otherwise, the surface temperature would be overestimated. To ease notation, we define

$$\Theta = \rho_i\, c_{p_i}\, h_{min} + \rho_s\, c_{p_s}\, h_s. \tag{7.15}$$

The change of heat flux with respect to temperature can be linearized:

$$\begin{aligned} \frac{dQ_b}{dT_i} &= \frac{Q_b^{(n+1)} - Q_b^{(n)}}{T_i^{(n+1)} - T_i^{(n)}} + \mathcal{O}(T_i^2), \\ \Rightarrow Q_b^{(n+1)} &= Q_b^{(n)} + \frac{dQ_b}{dT_i}\,(T_i^{(n+1)} - T_i^{(n)}). \end{aligned} \tag{7.16}$$

As in the present model the heat fluxes are assumed to be linear functions of temperature, the derivative $\frac{dQ_b}{dT_i}$ is a constant. For example, $\frac{dQ_c}{dT_i} = \frac{\kappa_i}{h_i}$. Eq. (7.13) is discretized, using (7.16), as

$$\begin{aligned} T_i^{(n+1)} - T_i^{(n)} &= \frac{\Delta t}{\Theta}\left(Q_b^{(n)} + \frac{dQ_b}{dT_i}\,(T_i^{(n+1)} - T_i^{(n)})\right) \\ \Rightarrow T_i^{(n+1)}\left(\frac{\Theta}{\Delta t} - \frac{dQ_b}{dT_i}\right) &= \left(\frac{\Theta}{\Delta t} - \frac{dQ_b}{dT_i}\right)T_i^{(n)} + Q_b^{(n)} \end{aligned} \tag{7.17}$$

where $T_i^{(n)}$ and $T_i^{(n+1)}$ denote the old and new sea ice temperature, respectively. Thus, the new surface temperature is given as

$$T_i^{(n+1)} = T_i^{(n)} + \frac{Q_b^{(n)}}{\frac{\Theta}{\Delta t} - \frac{dQ_b}{dT_i}}. \tag{7.18}$$

Snow cover

In a second step, the sea ice model is equipped with a snow cover. This changes the albedo properties, as snow has a slightly higher albedo (≈ 0.8) than ice. Also, the conductive heat flux through the ice is changed. The heat conductivity of snow is approximately 7-fold smaller than that of sea ice (cf. Table 7.1). Eq. (7.6) is changed to

$$Q_c = \begin{cases} 0 & \text{if} \quad T_s > T_f, \\ \dfrac{\bar{\kappa}}{h_i + h_s}(T_s - T_f), & \end{cases} \tag{7.19}$$

where $\kappa_s\,(\mathrm{W\,m^{-1}\,K^{-1}})$ is the heat conductivity of snow and $h_s\,(\mathrm{m})$ is the thickness of snow cover. If the surface temperature is above freezing, then first the snow is melted, then the ice. Snow melts according to

$$\frac{dh_s}{dt} = \frac{Q_a}{\rho_s\, L_{sn}}, \tag{7.20}$$

where $\rho_s\,(\mathrm{kg\,m^{-3}})$ is the density of snow and $L_{sn}\,(\mathrm{W\,s\,kg^{-1}})$ is the latent heat of fusion of snow. If the atmospheric heat flux is so large that it melts all the snow, then the remaining energy melts ice via (7.3). The source of snow is precipitation minus evaporation $P - E\,(\mathrm{mm\,m^{-1}\,d^{-1}})$ from PUMA, which, whenever the surface temperature drops below $0°C$, is considered to be snow:

$$\frac{dh_s}{dt} = \begin{cases} 0 & \text{if} \quad T_s \geq 0°C, \\ \dfrac{\rho_w}{\rho_s}(P - E) & \text{if} \quad T_s < 0°C, \end{cases} \tag{7.21}$$

Parameter	Symbol	Value	Reference
density of sea ice	ρ_i	$920\,\mathrm{kg\,m^{-3}}$	Kiehl et al. [1996, p. 139]
density of snow	ρ_s	$330\,\mathrm{kg\,m^{-3}}$	Kiehl et al. [1996, p. 139]
density of sea water[a]	ρ_w	$1030\,\mathrm{kg\,m^{-3}}$	
latent heat of fusion (ice)	L_i	$3.28 \times 10^5\,\mathrm{J\,kg^{-1}}$	Kiehl et al. [1996, p. 139]
latent heat of fusion (snow)	L_{sn}	$3.32 \times 10^5\,\mathrm{J\,kg^{-1}}$	Kiehl et al. [1996, p. 139]
heat conductivity in ice	κ_i	$2.03\,\mathrm{W\,m^{-1}\,K^{-1}}$	Kiehl et al. [1996, p. 139]
heat conductivity in snow	κ_s	$0.31\,\mathrm{W\,m^{-1}\,K^{-1}}$	Kiehl et al. [1996, p. 139]
specific heat of sea ice	c_{p_i}	$2070\,\mathrm{J\,kg^{-1}\,K^{-1}}$	Kiehl et al. [1996, p. 139]
specific heat of snow	c_{p_s}	$2090\,\mathrm{J\,kg^{-1}\,K^{-1}}$	Kiehl et al. [1996, p. 139]
specific heat of sea water	c_{p_w}	$4180\,\mathrm{J\,kg^{-1}\,K^{-1}}$	
ocean flux advection coefficient	c_o	$4\,(0.2)\,\mathrm{W\,m^{-2}\,K^{-1}}$ [b]	
freezing point of seawater [a]	T_f	271.25 K	
ocean water salinity	S_w	34.7 psu	
emissivity of sea ice surface	ε	0.945	King and Turner [1997, p. 70]
emissivity of snow surface	ε	0.975	King and Turner [1997, p. 70]

Table 7.1: Thermodynamic parameter values.
[a] at S=34.7
[b] Southern Ocean value 20 times larger than Arctic Ocean value.

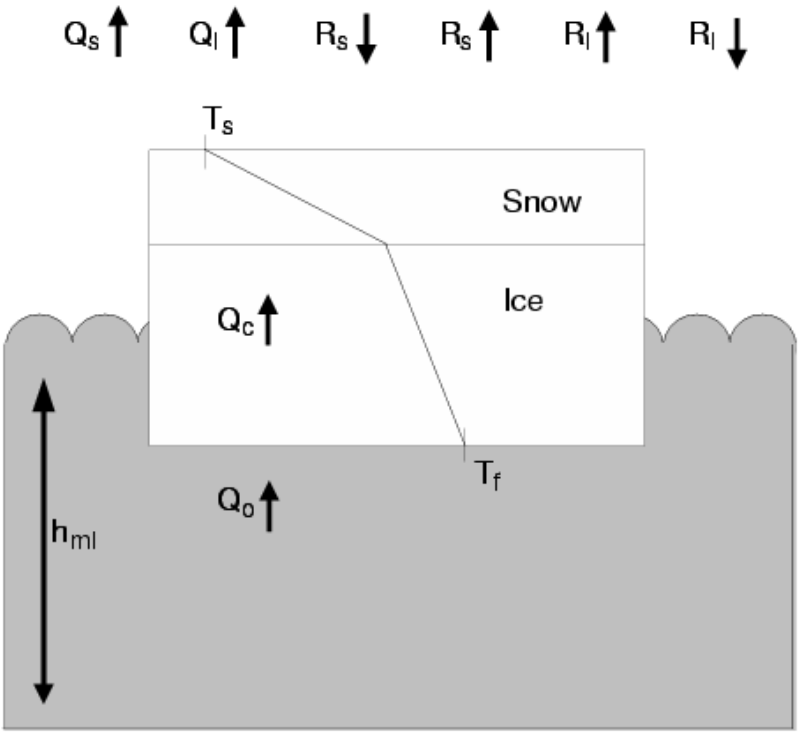

Figure 7.1: Schematic illustration of the temperature profile in the sea ice and the relevant heat fluxes. The atmospheric heat flux is the sum of sensible and latent heat flux (Q_s, Q_l), the incoming and reflected short wave radiation ($R_{s,\downarrow}$ $R_{s,\uparrow}$) and the long wave radiation (R_l). Ice growth and melting processes are additionally influenced by the conductive heat flux Q_c through the ice floe and the oceanic heat flux Q_o resulting from the temperature difference between water and ice. The mixed layer depth h_{ml} determines how much energy is available for ice formed from open water. The bottom temperature of the ice floe is set to the freezing temperature T_f. The sea ice surface temperature T_s is calculated according to the energy balance at the surface.

Maximal ice floe thickness

In this subsection, the maximal sea ice floe thickness is calculated. It is not desirable that the ice grows infinitely. Actually, this does not happen, as the conductive heat flux through the ice is decreased with increasing ice thickness and thus balances the oceanic heat flux at some maximal thickness of the ice floe. It follows from Eq. (7.3) that the maximal ice thickness, $h_{i,max}$, is reached when

$$h_i = h_{i,max} \iff Q_c + Q_o = 0, \tag{7.22}$$

thus, (using Eq. (7.8) and Eq. (7.19))

$$h_{i,max} = \frac{-(T_s - T_f)\kappa_i + c_o(T_d - T_f)h_s\kappa_i/\kappa_s}{c_o(T_d - T_f)}, \tag{7.23}$$

Fig. 7.2 shows the maximal sea ice thickness dependent on the surface temperature and the snow cover. The deep sea temperature is set to $T_d = 2°C$. For this calculation, the value of $c_o = 4\,W\,m^{-2}\,K^{-1}$ is used. Higher values of c_o lead to reduced maximal ice floe thicknesses. The presence of snow reduces the maximal sea ice thickness due to the significantly lower heat conductivity in snow compared to ice (cf. Table 7.1. As can be seen in Fig. 7.2, snow cover can even lead to negative sea ice thickness values. For example, at $T_s = -10°C$ and $h_s = 0.3\,m$, Eq. (7.22) balances at $h_{i,max} = -1\,m$. In this case, all ice under the snow cover will melt away. This effect is due to the crude parameterization of the oceanic heat flux.

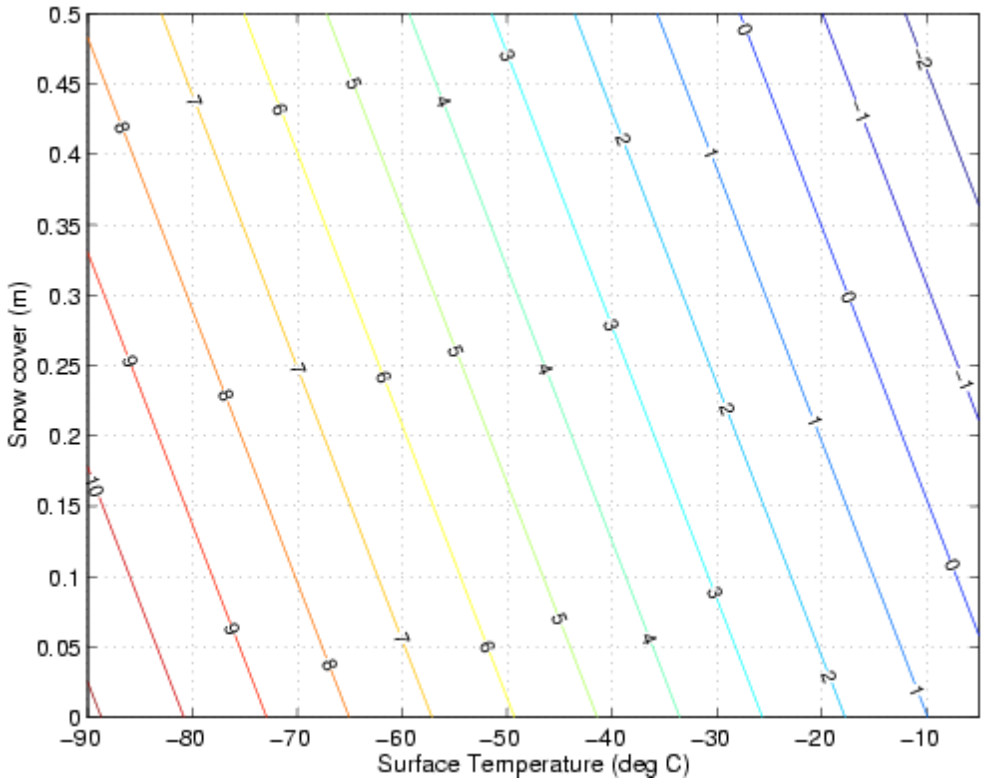

Figure 7.2: Maximal ice floe thickness at a deep sea temperature of 2°C.

Ocean heat flux parameterizations

Various parameterizations of the oceanic heat flux Q_{oc} have been proposed. *Hewitt et al.* [2000], who use the parameterization proposed by *Gordon et al.* [2000], state that they adjust the sea surface temperature (SST) such that the oceanic heat flux yields reasonable sea ice concentrations and thicknesses. An overview is given in Table 7.2. The parameterizations are illustrated in Fig. 7.3. In this work,the coefficient $c_o = 0.2\,\mathrm{W\,m^{-2}\,K^{-1}}$ parameterizes the advective oceanic heat transport such that the model yields realistic oceanic heat fluxes of $2\,\mathrm{W\,m^{-2}}$ in the central arctic and $10 - 20\,\mathrm{W\,m^{-2}}$ on the latitude of Spitzbergen [*Hibler and Zhang*, 1993].

Reference	Heat flux ($\mathrm{W\,m^{-2}}$)	Parameter values	Model type
this work[a]	$\mathrm{c\,(T_d - T_f)}$	$\mathrm{c} = 4(0.4)\,\mathrm{W\,m^{-2}\,K^{-1}}$	TD
Cattle and Crossley [1995]	$\rho_\mathrm{w}\,\mathrm{c_{p,w}}\,\gamma\,(\mathrm{SST} - \mathrm{T_f})\,/0.5\Delta\mathrm{z_1}$	$\gamma = 2.5 \times 10^{-3}\,\mathrm{m^2\,s^{-1}}$	TD
Birnbaum [1998]	$\rho_\mathrm{w}\,\mathrm{c_{p,w}}\,\gamma\,\mathrm{u_*}\,(\mathrm{SST} - \mathrm{T_f})$	$\gamma = 6 \times 10^{-3}$	D-TD
Lohmann et al. [1998]	$\mathrm{c\,(SST - T_f)}$	$\mathrm{c} = 200\,\mathrm{W\,m^{-2}\,K^{-1}}$	TD
Gordon et al. [2000]	$\mathrm{c\,(SST - T_f)}$	$\mathrm{c} = 20\,\mathrm{W\,m^{-2}\,K^{-1}}$	TD
Timmermann [2000]	$\rho_\mathrm{w}\,\mathrm{c_{p,w}}\,\gamma\,\mathrm{u_*}\,(\mathrm{SST} - \mathrm{T_f})$	$\gamma = 1.2 \times 10^{-2}$	D-TD
Timmermann [2000](b)	$\rho_\mathrm{w}\,\mathrm{c_{p,w}}\,\gamma\,(\mathrm{SST} - \mathrm{T_f})$	$\gamma = 10^{-4}\,\mathrm{m\,s^{-1}}$	D-TD

Table 7.2: Parameterizations of the oceanic heat flux. $\mathrm{T_d}, \mathrm{SST}$ and $\mathrm{T_f}$ denote the deep ocean, sea surface and freezing temperature, respectively. $\Delta\mathrm{z_1}$ denotes the thickness of the uppermost ocean box. The considered models are either thermodynamic models (TD) or dynamic-thermodynamic models (D-TD). The relative velocity between sea ice drift and ocean current is denoted by u_*. [a] value for the southern (northern) polar area.

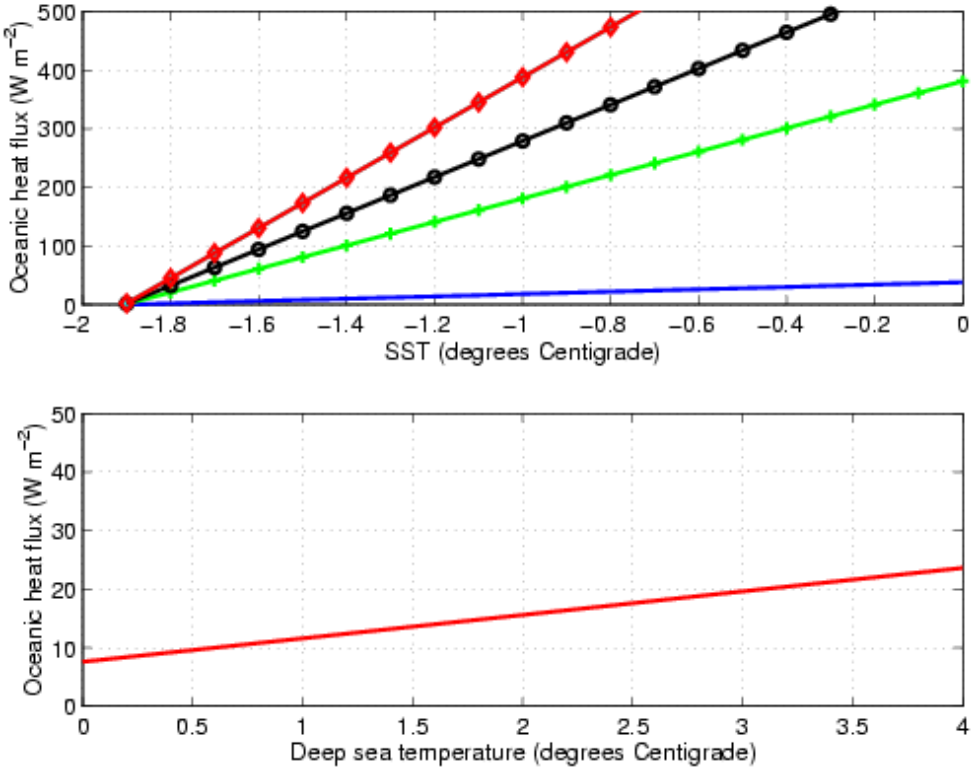

Figure 7.3: Parameterizations of the oceanic heat flux. Solid (top): *Gordon et al.* [2000]; Solid (bottom): this work (Southern Ocean value). Plusses: *Lohmann et al.* [1998]. Circles: *Birnbaum* [1998] with $u_* = 8.3 \times 10^{-3}$, following *Timmermann* [2000]. Diamonds: *Cattle and Crossley* [1995] with $\Delta z_1 = 50\,\mathrm{m}$, which then yields results equivalent to Timmermann [2000](b).

Output

Submodule-specific output is written to tape whenever the namelist parameter *NOUTPUT* is set to 1. An overview of output fields is given in Table 7. The scalar values are written in the diagnostic routine, i.e. every *NDIAG* time steps (default value every 5 days). The global fields are written every *NOUT* time steps (default value every 2 days).

Output field	Description	Code
	Scalar values written to fort.76 resp. icecover.srv	
xarc	Ice cover Arctic Ocean	951
xant	Ice cover Southern Ocean	952
xarcd	Mean ice thickness Arctic Ocean	953
xantd	Mean ice thickness Southern Ocean	954
xarcsnd	Mean snow depth Arctic Ocean	955
xantsnd	Mean snow depth Southern Ocean	956
xarcmf	Melt/freeze flux Arctic Ocean	961
xantmf	Melt/freeze flux Southern Ocean	962
xarcd.clim	Climatological mean ice thickness Arctic Ocean	963
xantd.clim	Climatological mean ice thickness Southern Ocean	964
	Global fields written to fort.75 resp. icedata.srv	
xicec	Ice concentration	210
xiced	Ice thickness	211
xsnow	Snow depth	141
xcliced2	Climatological ice thickness	911
xcmf	Cumulative melt/freeze flux	801
xheat	Heat flux received from atmosphere	701
xqoc	Heat flux received from deep ocean	702
xcflux	Conductive heat flux passed to ocean	703
xfluxrs	Ice growth flux saved for next time step	704
fxice2	Flux correction ice thickness	705
xlst	Land / Sea mask time dependent [a]	972

Table 7.3: Sea ice model output. [a] The land sea mask has to be written for every time step to avoid GRADS problems, as all other variables in *icedata.srv* are time-dependent.

Output field	Description	Code
ytoc	SST	851
yhmix	MLD	853
yclim2	Climatological SST	721
ycdpt2	Climatological MLD	722
yfsst2	Flux correction SST	711
yfdpt2	Flux correction MLD	712
ytbottom	Deep ocean temperature	852
yqoc	Heat flux from deep ocean	702

Table 7.4: Mixed layer model output written to fort.31 resp. oceandata.srv.

Part V

Bibliography

Bibliography

[Apel (1987)] Apel, J. R., Principles of Ocean Physics, *Academic Press*, Int. Geophys. Ser., **38**, 1987.

[Beckmann and Birnbaum (2001)] Beckmann, A. and Birnbaum, G., Cryosphere : Coupled Sea Ice - Ocean Models, *Academic Press*, Encyclopedia of Ocean Sciences, 2001.

[Birnbaum (1998)] Numerical modelling of the interaction between atmosphere and sea ice in the Arctic marginal ice zone, *Alfred Wegener Institute for Polar and Marine Research*, PhD-thesis, 1998.

[Buizza et al. (1999)] Buizza, R., Miller, M. and Palmer, T. N., Stochastic representation of model uncertainties in the ECMWF Ensemble Prediction System, *Q. J. R. Meteorol. Soc.*, **125**, 2887–2908, 1999.

[Cattle and Crossley (1995)] Cattle, H. and Crossley, J., Modelling Arctic Climate Change, *Phil. Trans. Roy. Soc. Lon. A*, **352**, 201–213, 1995.

[Dommenget and Latif (2000)] Dommenget, D. and Latif, M., Generation of SST anomalies in the midlatitudes, *Max-Planck-Institut Report*, **304**, 2000.

[Eliassen et al. (1970)] Eliassen, E., Machenhauer, B., and Rasmusson, E., On a numerical method for integration of the hydrodynamical equations with a spectral representaion of the horizontal fields, *Inst. of Theor. Met., Univ. Copenhagen*, 1970.

[García-Ojalvo and Sancho (1999)] García-Ojalvo, J. and Sancho, J. M., Noise in spatially extended systems, *Springer-Verlag, New-York*, 1999.

[Gaspar (1988)] Gaspar, P., Modeling the seasonal cycle of the upper ocean, *J. Phys. Oceanogr.*, **18**, 161–180, 1988.

[Gordon et al. (2000)] Gordon, C. et al. The simulation of SST, sea ice extents and ocean heat transports in a version of the Hadley Centre coupled model without flux adjustments, *Clim. Dyn.*, **16**, 147–168, 2000.

[Haltiner and Williams (1982)] Haltiner, G. J. and Williams, R. T., Numerical Prediction and Dynamic Meteorology, *John Wiley and Sons, New York*, 1982.

[Hewitt (2000)] Hewitt, G., The genetic legacy of the Quaternary ice ages, *Nature*, **405**, 907–913, 2000.

[Hibler and Zhang (1993)] Hibler, W. D. III and Zhang, J. Interannual and climatic characteristics of an ice ocean circulation model, *Springer-Verlag New York*, NATO ASI Series Global and Environmental Change, 1993.

[Hoskins and Simmons (1975)] Hoskins, B. J. and Simmons, A. J., A multi-layer spectral method and the semi-implicit method, *Q. J. R. Meteorol. Soc.*, **101**, 637–655, 1975.

[Houtekamer and Derome (1995)] Houtekamer, P. L. and Derome, J., Methods for ensemble prediction, *Mon. Wea. Rev.*, **123**, 2181–2196, 1995.

[Houtekamer et al.(1996)] Houtekamer, P.L., Lefaivre, L., Derome, J., Ritchie, H. and Mitchell, H., A system simulation approach to ensemble prediction, *Mon. Wea. Rev.*, **124**, 1225–1242, 1996.

[Karaca and Müller (1991)] Karaca, M. and Müller, D., Mixed-layer dynamics and buoyancy transports, *Tellus*, **43**, 350–365, 1991.

[Kiehl et al. (1996)] Kiehl, J. T., Hack, J. J., Bonan, iG. B., Boville, iB. A., Briegleb, B. P., Williamson, D. L. and Rasch, P. J., Description of the NCAR Community Climate Model (CCM3), *National Centre for Atmospheric Research*, 1996.

[King and Turner (1997)] King, J. C. and Turner, J., Antarctic Meteorology and Climatology, *Cambridge University Press*, 1997.

[Kraus (1967)] Kraus, E. B. and Turner, J. S., One-dimensional model of the seasonal thermocline II. The general theory and its consequences. *Tellus*, **19**, 98–105, 1967.

[Lohmann and Gerdes (1998)] Lohmann, G. and Gerdes, R., Sea Ice Effects on the Sensitivity of the Thermohaline, *J. Clim.*, **11**, 2789–2803, 1998.

[Lorenzo and Pérez-Muñuzuri (1999)] Lorenzo, M. N. and Pérez-Muñuzuri, V., Colored noise-induced chaotic array synchronization, *Phys. Rev. E*, **60**, 2779–2787, 1999.

[Lorenzo and Pérez-Muñuzuri(2001)] Lorenzo, M.N. and Pérez-Muñuzuri, V., Influence of low intensity noise on assemblies of diffusively coupled chaotic cells, *Chaos*, *11*, 371–376, 2001.

[Lorenzo et al.(2002)] Lorenzo, M.N., Santos M.A. and Pérez-Muñuzuri, V., Spatiotemporal stochastic forcing effects in an ensemble consisting of arrays of diffusively coupled Lorenz cells, *submitted to Phys. Rev. E*, 2002.

[Lunkeit(2001)] Lunkeit, F., Synchronization experiments with an atmospheric global circulation model, *Chaos*, *11*, 47–51, 2001.

[Molteni et al.(1996)] Molteni, F., Buizza, R., Palmer T.N. and Petroliagis, T., The ECMWF ensemble prediction system: Methodology and validation, *Q.J.R. Meteorol. Soc.*, *122*, 73–120, 1996.

[Orszag (1970)] Orszag, S. A., Transform method for calculation of vector coupled sums, *J. Atmos. Sci.*, **27,** 890-895.

[Parkinson and Washington (1979)] Parkinson, C. L. and Washington, W. M., A large-scale numerical model of sea ice, *J. Geophys. Res.*, **84**, 311–337, 1979.

[Phillips (1957)] Phillips, N. A., A coordinate system having some special advatages for numerical forecasting, *J. Meteorology*, **14**, 184–185, 1957.

[Santos and Sancho(2001)] Santos, M.A. and Sancho, J.M., Front dynamics in the presence of spatiotemporal noises, *Phys. Rev. E*, *64*, 016129(1)–016129(11), 2001.

[Semtner (1976)] Semtner, A. J. Jr., A Model for the Thermodynamic Growth of Sea Ice in Numerical Investigations of Climate, *J. Physic. Oceanogr.*, **3**, 379–389, 1976.

[Simmons et al.(1978)] Simmons, A. J., B. J. Hoskins, and D. M. Burridge, 1978: Stability of the semi-implicit method of time integration. *Mon. Wea. Rew.*, **106,** 405–412.

[Simmons and Burridge (1981)] Simmons, A. J., and D. M. Burridge, 1981: An Energy and Angular-Momentum Conserving Vertical Finite-Difference Scheme and Hybrid Vertical Coordinates. *Mon. Wea. Rew.*, **109,** 758–766.

[Smith et al.(1999)] Smith, L.A., Ziehmann, C. and Fraedrich, K., Uncertainty dynamics and predictability in chaotic systems, *Q.J.R. Meteorol. Soc.*, *125*, 2855–2886, 1999.

[Timmermann (2000)] Timmermann, R., Wechselwirkungen zwischen Eis und Ozean im Weddelmeer, *University of Bremen*, 2000.

[Toth and Kalnay(1993)] Toth, Z. and Kalnay, E., Ensemble forecasting at NMC: The generation of perturbations, *Bull. Amer. Meteor. Soc.*, *74*, 2317–2330, 1993.

[UNESCO (1978)] Eighth report of the joint panel on oceanographic tables and standards, *UNESCO Technical Papers in Marine Science*, **28**, 1978.

[Whitaker and Lougue(1998)] Whitaker, J.S. and Lougue, A.F., The relationship between ensemble spread and ensemble mean skill, *Mon. Wea. Rev.*, *126*, 3292–3302, 1998.

[Wilks(1995)] Wilks, D.S., *Statistical methods in the atmospheric sciences*, Academic Press, New-York, 1995.